SUPPORTING INFORMATION

New dioxaborolane chemistry enables [^{18}F]-positron-emitting, fluorescent [^{18}F]-multimodality biomolecule generation from the solid-phase

Erik A. Rodriguez[†,#], Ye Wang[§,#], Jessica L. Crisp[†], David R. Vera[‖], Roger Y. Tsien[†,‡], and Richard Ting[†,§,*]

[†]Department of Pharmacology, University of California, San Diego, La Jolla, CA 92093, USA.
[§]Molecular Imaging Innovations Institute (MI3), Department of Radiology, Weill Cornell Medicine, New York, NY 10065, USA.
[‖]Department of Radiology, University of California, San Diego, La Jolla, CA 92093, USA.
[‡]Howard Hughes Medical Institute, La Jolla, CA 92093, USA.
[#]E.A.R and Y.W. contributed equally to this work.

Table of Contents:

Schemes:

Figures:

Videos

Solid-phase preparation of [$^{18/19}$F]/ near infrared fluorescent (NIRF) labeled mAbs for multimodality imaging.

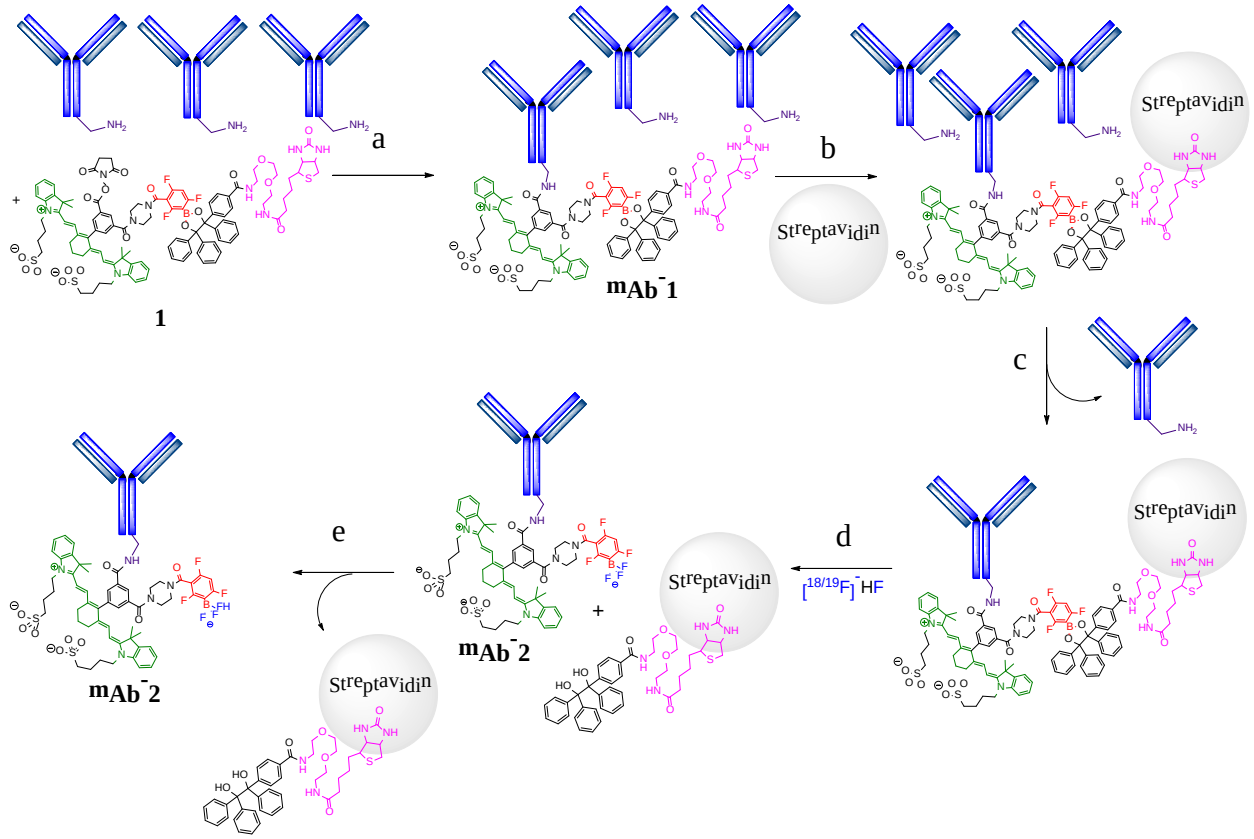

Scheme S1. Generation of a mAb-**1** bound to streptavidin-agarose and radioactive fluoride triggered release of mAb-**2**.

(a) Amide formation is achieved between a mAb lysine amino acid and **1** through NHS-ester mediated coupling (PBS + 4-methylmorpholine (NMM), pH 7.5) resulting in mAb-**1**. (b) Streptavidin-agarose is introduced, which captures solution-phase, biotin-bearing mAb-**1**. (c) Unreacted mAb is removed from mAb-**1**-bound streptavidin-agarose by washing with H_2O. (d) Reacting mAb-**1**-bound streptavidin-agarose with fluoride achieves two simultaneous events: 1) The generation of the trifluoroborate, mAb-**2** and 2) The release of mAb-**2** from the solid-phase. (e) Unreacted mAb-**1** remains bound to the streptavidin-agarose, which can be reused in future syntheses of mAb-**2**.

1. Synthetic Chemistry

Small molecule synthesis and characterization, biotinylated-pinacol protected boronate/NIRF probe synthesis (1). The synthesis of a boronated, [$^{18/19}$F]-PET/NIRF agent, **1**, that is protected with a biotinylated pinacol is described in an 8 step convergent synthesis (Scheme S2). The final yield of **1** is 0.4%. Two under-optimized chemical steps contribute to the low yield: 1) Unwanted side products from the photochemical syntheses of mono-carboxy pinacol (**iii**) and 2) inefficient loading of carboxy pinacol onto electron withdrawing boronates during pinacol-boronate ester syntheses (**iv**).

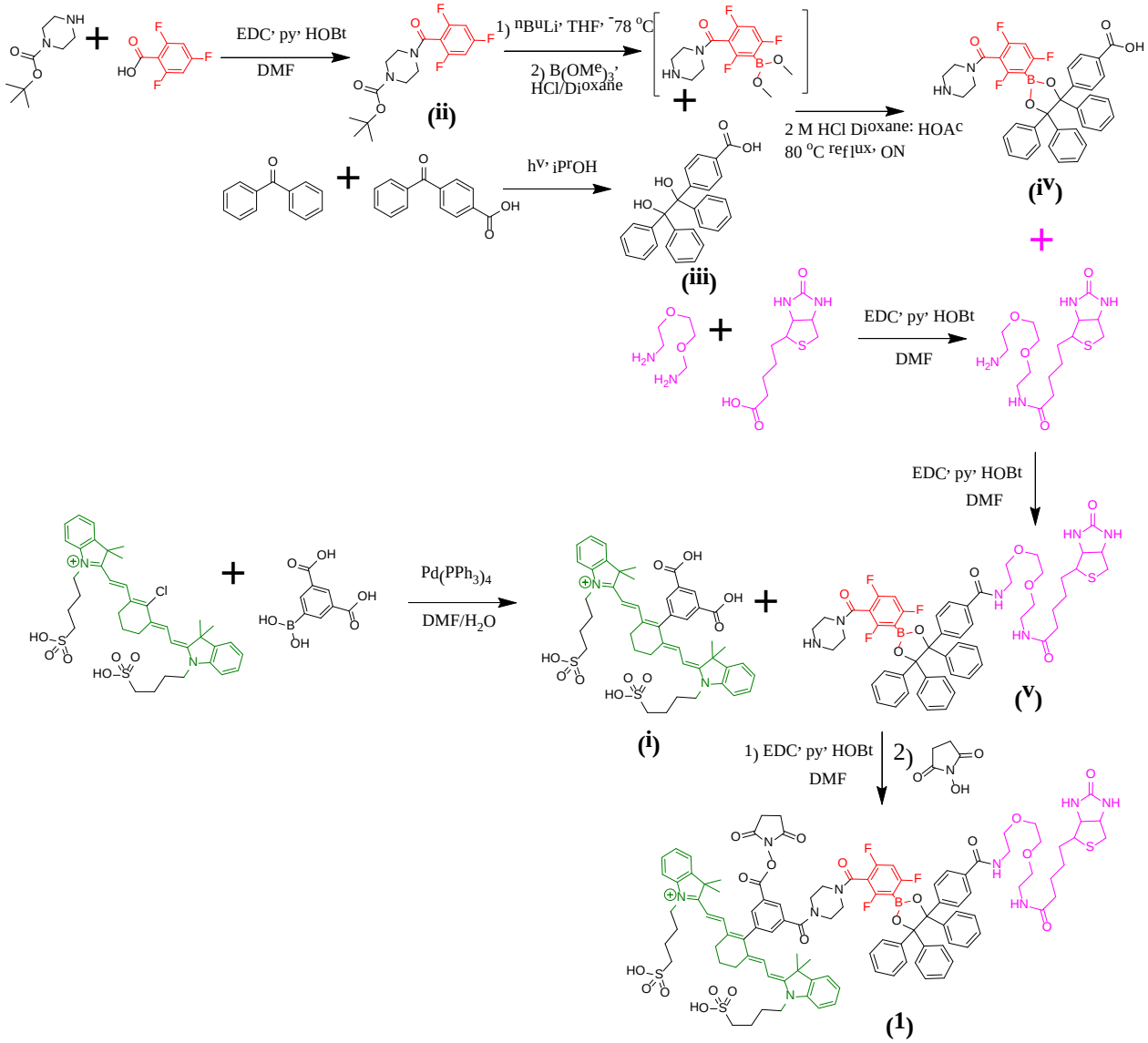

Scheme S2. Synthesis of a boronated, [$^{18/19}$F]-PET/NIRF precursor, **1**, modified with a biotin.

The boron based fluoride trap is shown in orange, the Cy7 NIR fluorophore is shown in green, and the biotin moiety is shown in pink.

1.1 General synthetic methods. Chemicals were purchased from Oakwood Chemical, Aldrich, Combi-blocks, Strem, and Alfa Aesar. Analytical, reverse phase HPLC were performed on a Agilent 1100 Series HPLC with a Phenomenex Luna C18(2) 100 Å, 250 cm x 4.60 mm I.D. 5 μm reverse phase column (00G-4252-E0), with a 20 min, a10-90% H_2O:acetonitrile (ACN) (0.05% TFA) gradient and a flow rate of 1 mL/min (unless stated otherwise). Preparative HPLC was performed on a Agilent 1200 Series HPLC equipped with a mass spectrometer (HPLC-MS, Agilent LC/MSD trap XCT) on a Phenomenex Luna C18(2) 100 Å, 250 cm x 21.20 mm I.D. 10 μm reverse phase column (00G-4253-P0 AX), with a 20 min, a10-90% H_2O:ACN (0.05% TFA) gradient and a flow rate of 15 mL/min. ^{1}H-NMR were performed on a Jeol 500 MHz spectrometer. High-resolution mass spectrometry was performed at the University of California San Diego (UCSD) Chemistry and Biochemistry Small Molecule/Chemical Mass Spectrometry Facility.

1.2 Synthesis of dicarboxyphenyl modified cyanine7 dye IR-783 (i). Palladium-catalyzed cross coupling was used in the synthesis of the cyanine7 fluorophore[44]. Reagents were added to a 25 mL round bottom flask (rbf) with a magnetic stir bar in the following order: IR-783 (500 mg, 0.67 mmols, Sigma-Aldrich 543292), 3,5-dicarboxyphenyl boronic acid (330 mg, 1.6 mmols, Combi Blocks BB-3936), dimethylformamide (10 mL), and H_2O (10 mL). The reaction was started with the addition of tetrakis(triphenylphosphine)palladium(0) (100 mg, 0.09 mmols, Strem 46-2150m) and refluxed for 4.5 hours at 120 °C. The contents of the rbf were concentrated *in vacuo* to a solid, resuspended in DMF, and loaded on a preparative reverse phase HPLC column. Fractions containing **i** were lyophilized as H_2O/ACN mixtures to give **i** as a solid green compound (303 mg, 0.35 mmols, 52% yield).

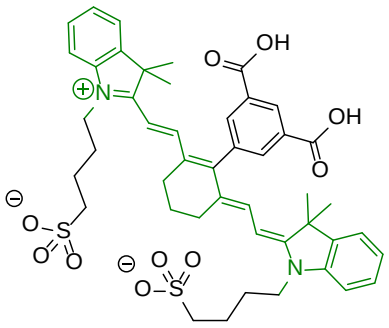

i

Chemical Formula: $C_{46}H_{51}N_2O_{10}S_2^-$
Exact Mass: 855.2991
Molecular Weight: 856.0351
m/z: 855.2985 (100.0%), 856.3019 (49.8%), 857.3052 (12.1%)

^{1}H NMR (DMSO-d6, 500 MHz, 21 °C): δ 8.23, 7.60, 7.35, 7.16, 6.04, 4.04, 3.86, 1.76, 1.63. HRMS (ESI) calculated for $C_{46}H_{51}N_2O_{10}S_2^-$ $(M)^-$: 855.2991, found 855.2991 (< Δ 0.1 ppm). Spectrophotometric constants were determined in Dulbecco's phosphate-buffered saline (1x DPBS): λ_{max} = 754 nm, ε_{754} = 191,000 cm^{-1} M^{-1}, λ_{max} (shoulder) = 689 nm, $\varepsilon_{689\ (sh)}$ = 60,000 cm^{-1} M^{-1}. Analytical reverse phase HPLC-MS retention time with a a10-90% H_2O:ACN (0.05% TFA), 20 min gradient, 1 mL/min: 12.6 min. Preparative HPLC retention time with a10-90% H_2O:ACN (0.05% TFA) 40 min gradient: 24-27 min.

^{1}H NMR (DMSO-d6, 500 MHz, 21 °C):

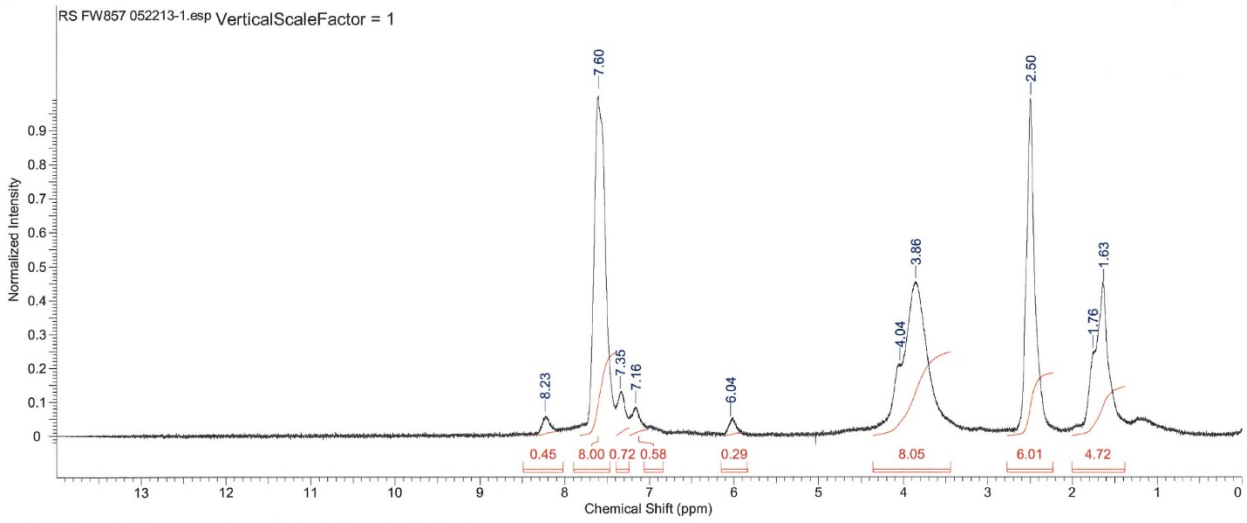

HPLC-MS$^+$: H_2O:ACN (0.05% TFA), 20 min gradient, 1 mL/min flow, det. 280, 215,780, 650 nm:

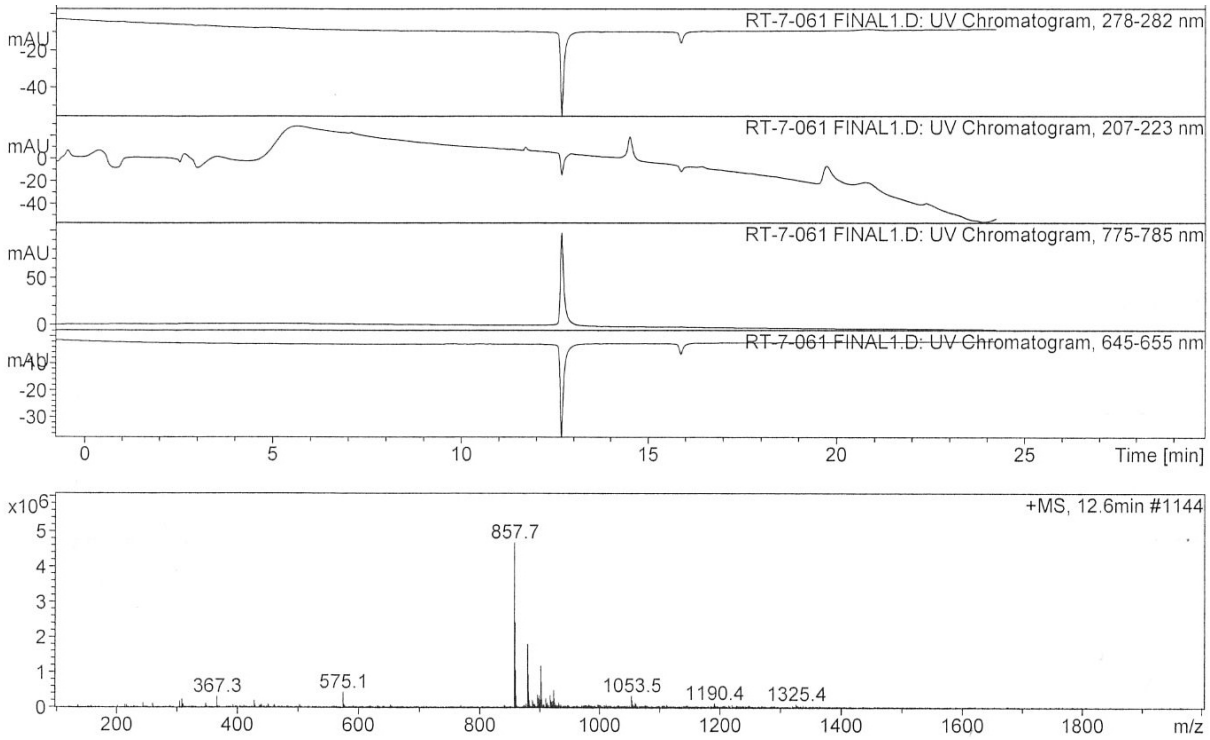

HRMS-ESI$^-$ (negative mode):

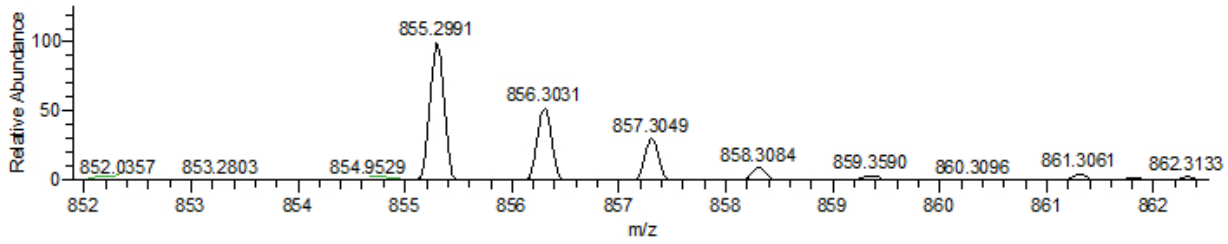

1.3 Synthesis of tert-butyl 4-(2,4,6-trifluorobenzoyl)piperazine-1-carboxylate (ii). The following reagents were added to a 100 mL rbf: 2,4,6-Trifluorobenzoic acid (10 g, 57 mmols, Oakwood Chemical 002067), tert-butyl 1-piperazinecarboxylate (10.4 g, 55.8 mmols, Oakwood Chemical 021572), and HOBt monohydrate (4 g, 26 mmols). The contents of the rbf were dissolved with 20 mL DMF and 1.6 mL of pyridine before condensation was started with N-3(-dimethylaminopropyl)-N'-ethyl carbodiimide hydrochloride (EDC) (10 g, 104 mmols). The reaction proceeded for 2 hours at 40 °C before being transferred to a 1 L separatory funnel containing 200 mL $CHCl_3$ and 300 mL H_2O. The $CHCl_3$ layer was washed 3x with H_2O, dried over anhydrous sodium sulphate, and concentrated *in vacuo* to give 18.8 g of **ii** (18.8 g, 55 mmols, 97% yield). The purity of **ii** after extraction is sufficient for n-butyl lithium based carbanion formation.

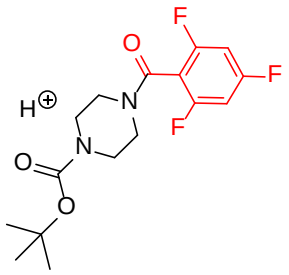

ii

Chemical Formula: $C_{16}H_{20}F_3N_2O_3^+$
Exact Mass: 345.1421
Molecular Weight: 345.3363
m/z: 345.1426 (100.0%), 346.1460 (17.3%), 347.1493 (1.4%)

^{1}H NMR (DMSO-d6, 500 MHz, 21 °C): δ 7.36 (br, Ar-H), 3.64 (CH_2), 3.39 (CH_2), 3.27 (CH_2), 1.40 (CH_3). HRMS (ESI) calculated for $C_{16}H_{19}F_3N_2O_3^+$ $(M+H)^+$: 345.1421, found 345.1424 (Δ 0.9 ppm). Analytical HPLC-MS retention time with a a10-90% H_2O:ACN (0.05% TFA), 20 min gradient: 17.5 min. Preparative HPLC with a a10-90% H_2O:ACN (0.05% TFA), 40 min gradient: 28-30 min.

^{1}H NMR (DMSO-d6, 500 MHz, 21 °C):

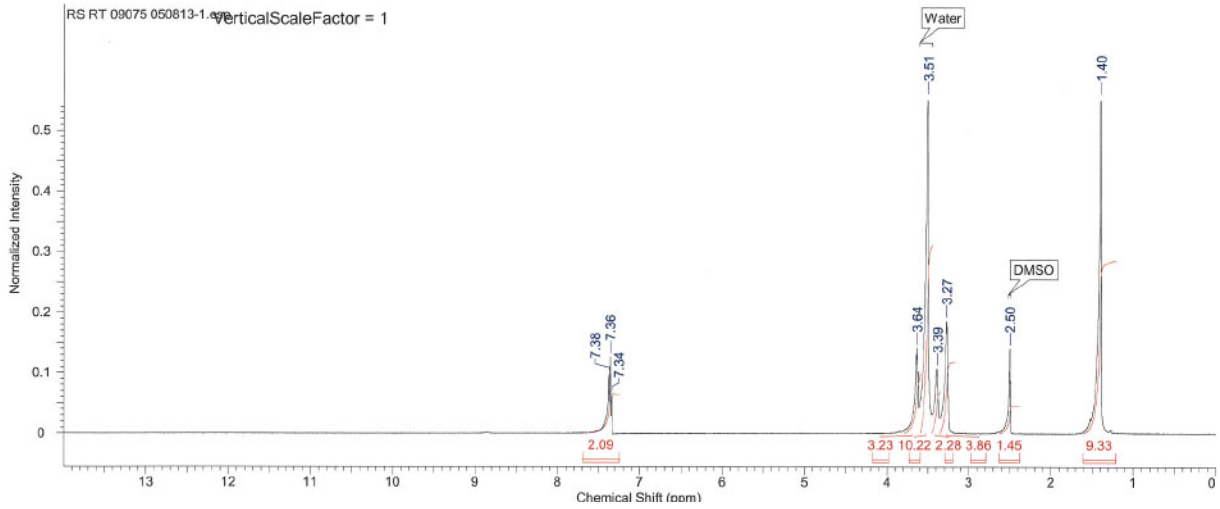

HPLC-MS: H_2O:ACN (0.05% TFA), 20 min gradient, 1 mL/min flow, det. 215 nm 280 nm:

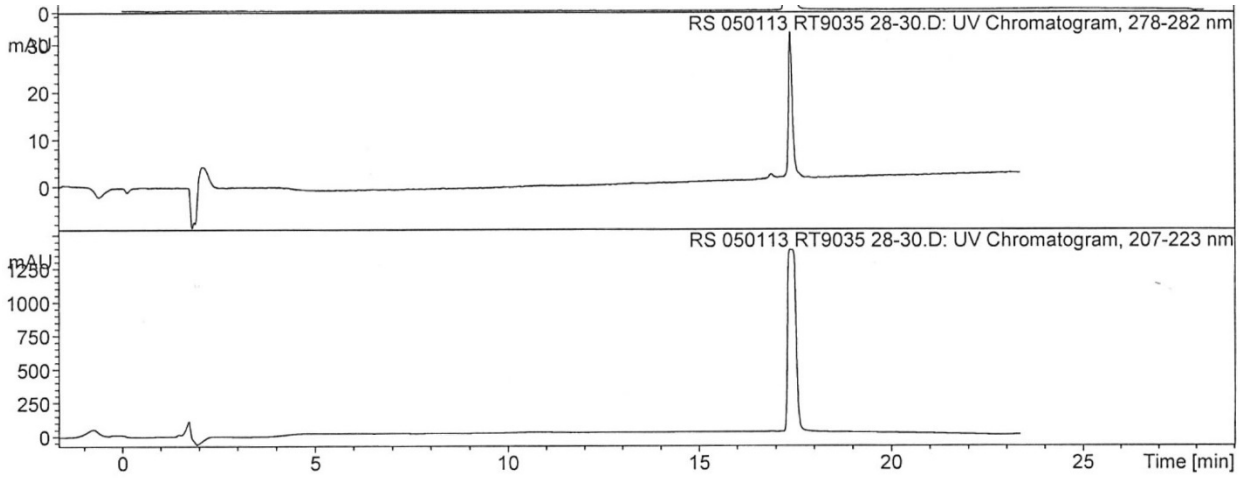

HRMS-ESI$^+$:

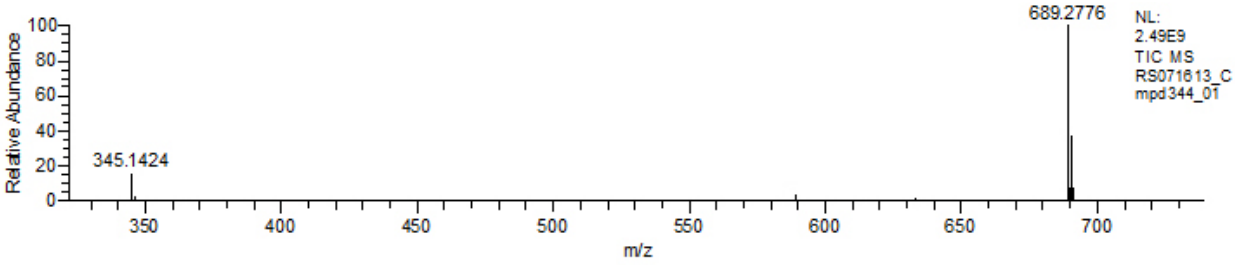

1.4 Synthesis of 4-(1,2-dihydroxy-1,2,2-triphenylethyl)benzoic acid (iii). Benzophenone (5 g, 27 mmols) and 4-Benzyl benzoic acid (4 g, 15 mmols, Alfa Aesar A14993) were placed in a 500 mL Erlenmeyer flask and dissolved with 300 mL iPrOH. This solution was transferred to a 4 °C, H_2O-cooled low-pressure mercury-vapor photoreactor. Reagents were irradiated at 254 nm for 2.5 hours, the reaction was transferred to a 500 mL rbf, and the resulting products were concentrated *in vacuo*. The resulting mixture containing **iii**, Benzopinacol, 4,4'-(1,2-dihydroxy-2,2-diphenylethane-1,1-diyl)dibenzoic acid, and 4,4'-(1,2-dihydroxy-1,2-diphenylethane-1,2-diyl)dibenzoic acid was reacted as an unpurified mixture in the next step to give **iv**. For NMR studies, **iii** was dissolved in DMF and purified by reverse phase HPLC.

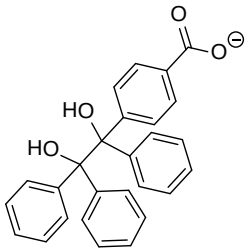

iii

Chemical Formula: $C_{27}H_{21}O_4^-$
Exact Mass: 409.1445
Molecular Weight: 409.4538
m/z: 409.1440 (100.0%), 410.1473 (29.2%), 411.1507 (4.1%)

^{1}H NMR (DMSO-d6, 500 MHz, 21 °C): δ 12.81 (COOH), 7.32 (Ar-H), 7.10 (Ar-H), 6.14 (Ar-H), 4.06 (OH). HRMS (ESI) calculated for $C_{27}H_{21}O_4$ (M^-): 409.1445, found 409.1434 (Δ 2.7 ppm). Analytical HPLC-MS retention time using a10-90% H_2O:ACN (0.05% TFA), 20 min gradient, 1 mL/min: 18.1 min. Preparative HPLC on a a10-90% H_2O:ACN (0.05% TFA) 20 min gradient: 19-20 min.

^{1}H NMR (DMSO-d6, 500 MHz, 21 °C):

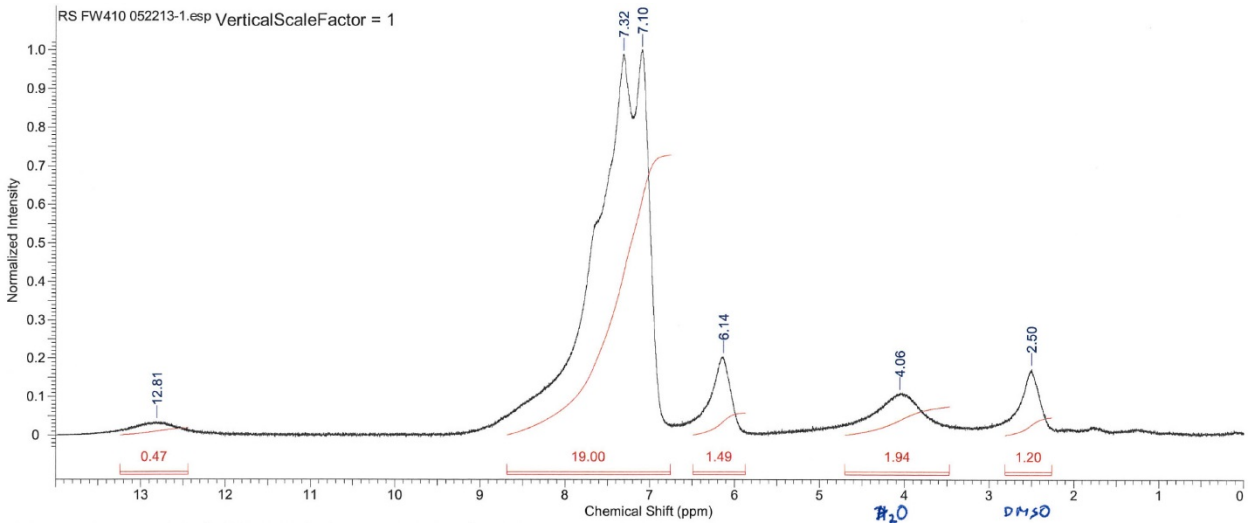

HPLC: H_2O:ACN (0.05% TFA), 20 min gradient, 1 mL/min flow, det. 215 nm and 280 nm:

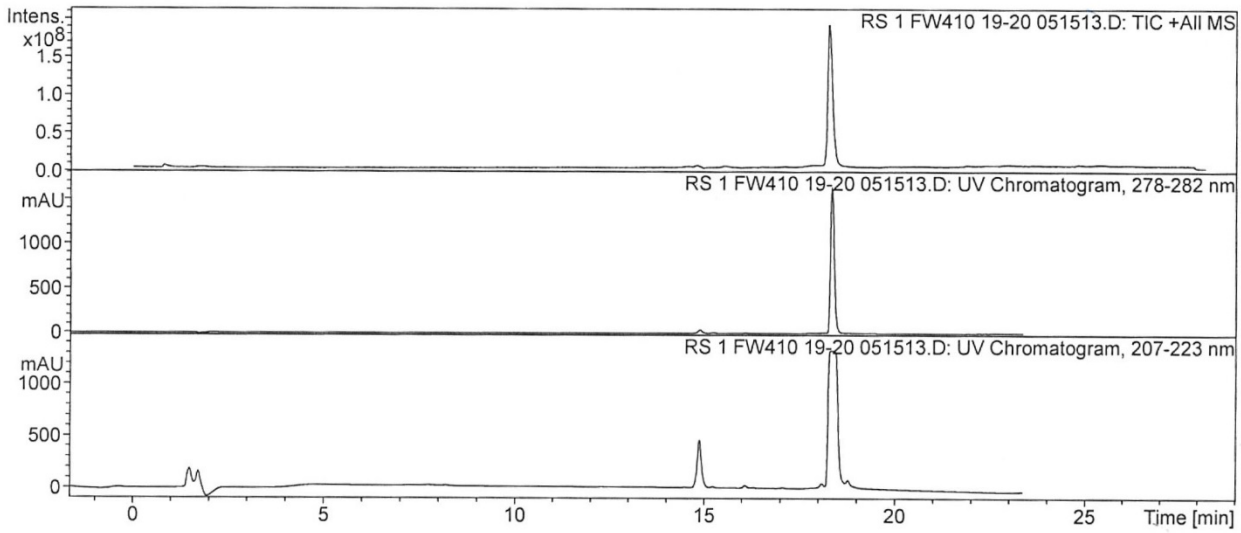
Intens.
x10^8
1.5
1.0
0.5
0.0
RS 1 FW410 19-20 051513.D: TIC +All MS
mAU
1000
500
0
RS 1 FW410 19-20 051513.D: UV Chromatogram, 278-282 nm
mAU
1000
500
0
RS 1 FW410 19-20 051513.D: UV Chromatogram, 207-223 nm
0
5
10
15
20
25
Time [min]

HRMS-ESI$^-$:

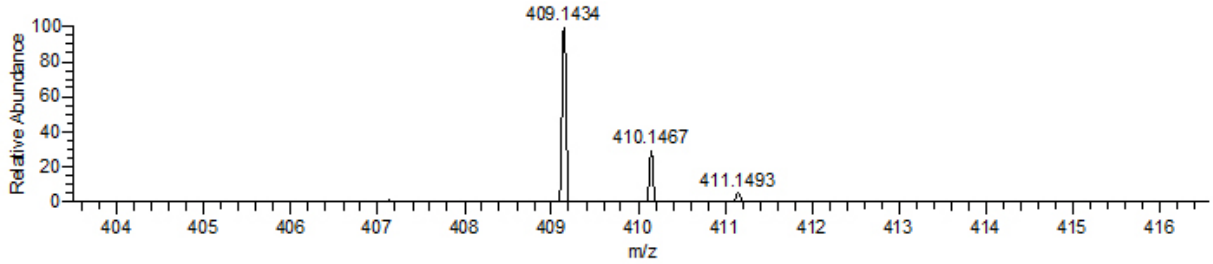
409.1434
410.1467
411.1493
Relative Abundance
100
80
60
40
20
0
404
405
406
407
408
409
410
411
412
413
414
415
416
m/z

1.5 Synthesis of 4-(4,5,5-triphenyl-2-(2,4,6-trifluoro-3-(piperazine-1-carbonyl)phenyl)-1,3,2-dioxaborolan-4-yl)benzoic acid (iv). **ii** (3 g, 8.72 mmols) was added to a flame-dried, nitrogen-flushed 100 mL rbf with a magnetic stir bar. **ii** was dissolved in 40 mL tetrahydrofuran and cooled to -78 °C under a nitrogen atmosphere. nBuLi (12 mL, 19.2 mmols, 1.6 M in hexanes) was added by syringe over a 4 min period, inducing a solution color change from a clear light yellow to an opaque orange. The reaction was incubated at -78 °C for 25 min before trimethyl borate (3 g, 8.72 mmols) was added by syringe over a 1 min period at -78 °C. Boronation was allowed to proceed for 30 min at -78 °C before the reaction was quenched with the addition of 20 mL of 4 M HCl in dioxane. The reaction was transferred to a 500 mL rbf and concentrated *in vacuo* to foam. ~3 g of pinacol mixture (**iii**) was added to the resulting foam, which was then dissolved in a solution containing 6 mL of 4 M HCl in dioxane and 12 mL glacial acetic acid (HOAc). This solution was heated to 80 °C for 16 hours and was concentrated to an oil. 15 mL MeOH was added to the oil and the resulting suspension was centrifuged at 3,000 rcf for 5 min. The supernatant containing **iv** was decanted off the pellet, transferred to a 500 mL rbf and concentrated to foam. The concentrate was mixed with 150 mL H_2O, triturated, and centrifuged at 3,000 rcf for 5 min. The resulting aqueous supernatant was decanted and the pellet, containing **iv**, was suspended in 5 mL DMF for HPLC purification. Fractions containing **iv** were lyophilized to give **iv** as a solid white compound (717 mg, 1.1 mmols, 13% yield) that is stored at -78 °C.

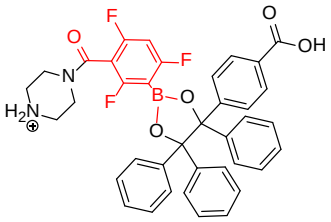

iv
Chemical Formula: $C_{38}H_{31}BF_3N_2O_5^+$
Exact Mass: 663.2273
Molecular Weight: 663.4688
m/z: 663.2278 (100.0%), 664.2312 (41.1%), 662.2314 (24.8%), 663.2348 (10.2%)

^{1}H NMR (DMSO-d6, 500 MHz, 21 °C): δ 12.97, 9.01, 7.69, 7.51, 7.34, 7.14, 3.87, 3.58, 3.23, 3.09. HRMS (ESI) calculated for $C_{38}H_{31}BF_3N_2O_5^+$ $(M+H)^+$: 663.2273, found 663.2272 (Δ 0.1 ppm). Analytical HPLC-MS retention time with a a10-90% H_2O:ACN (0.05% TFA), 20 min gradient, 1 mL/min: 14.8 min. Preparative HPLC with a10-90% H_2O:ACN (0.05% TFA) 20 min gradient: 14.8-16 min.

^{1}H NMR (DMSO-d6, 500 MHz, 21 °C):

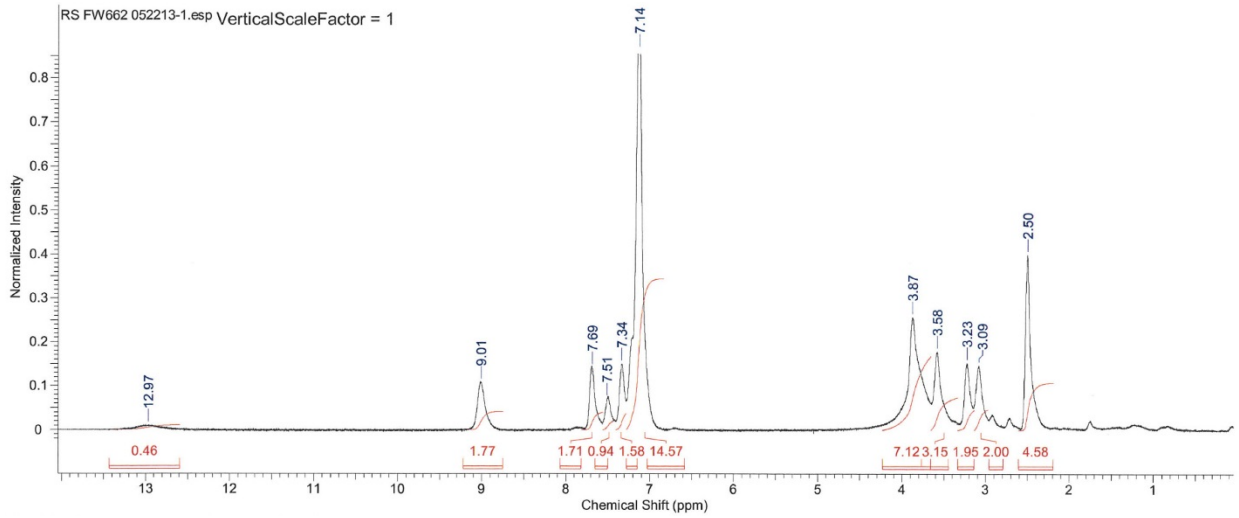

HPLC-MS: H_2O:ACN (0.05% TFA), 20 min gradient, 1 mL/min flow, det. 215 nm 280 nm:

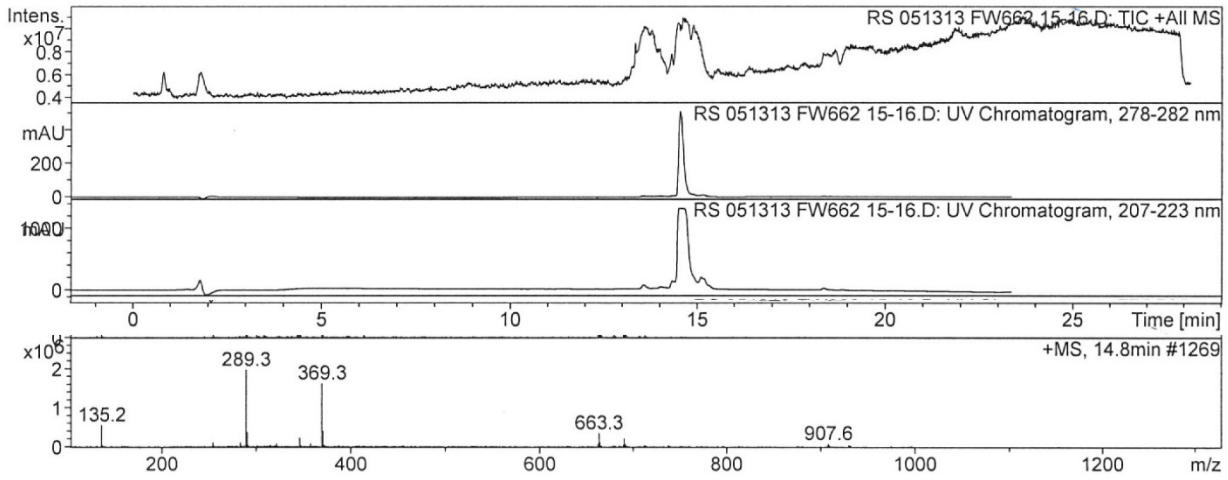

HRMS-ESI^{+}:

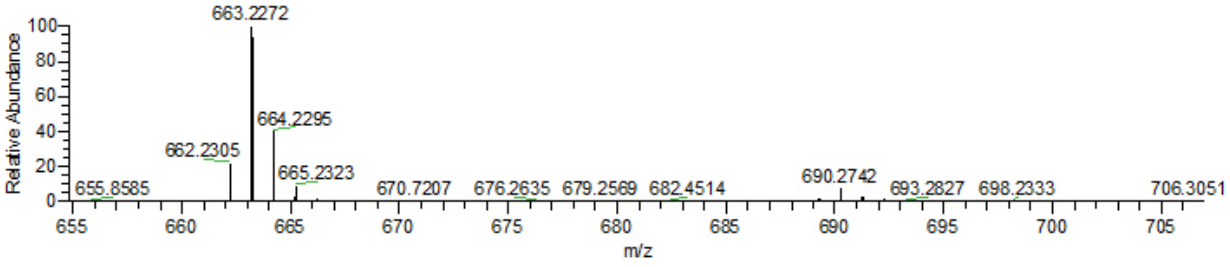

1.6 Synthesis of 4-(4,5,5-triphenyl-2-(2,4,6-trifluoro-3-(piperazine-1-carbonyl)phenyl)-1,3,2-dioxaborolan-4-yl)benzoic acid (v). The reagents were added to a 25 mL rbf in the following order: Amine PEG_2-Biotin (388 mg, Pierce 21346), **iv** (156 mg, 246 µmol), DMF (1 mL), N-Hydroxybenzotriazole (31 mg, 202 µmol), pyridine (200 µL), and 1-Ethyl-3-(3-dimethylaminopropyl)carbodiimide (EDC) (150 mg, 785 µmol). This reaction was incubated for 16 hours. The 1 mL reaction was loaded directly on a reverse phase HPLC. Fractions containing **v** were lyophilized as H_2O:ACN mixtures to give **v** as a solid white compound (80.1 mg, 78.7 µmols, 12% yield) that is stored at -78 °C.

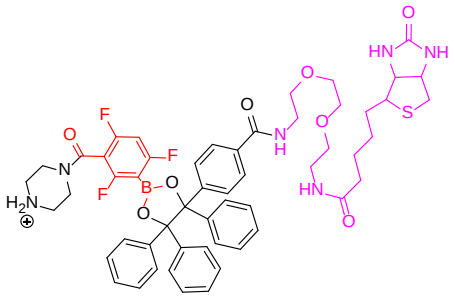

v

Chemical Formula: $C_{54}H_{59}BF_3N_6O_8S^+$
Exact Mass: 1019.4155
Molecular Weight: 1019.9523
m/z: 1019.4160 (100.0%), 1020.4194 (58.4%), 1018.4197 (24.8%), 1021.4227 (16.7%), 1019.4230 (14.5
Sodium Salt:
Chemical Formula: $C_{54}H_{58}BF_3N_6NaO_8S^+$
Exact Mass: 1041.40

^{1}H NMR (DMSO-d6, 500 MHz, 21 °C): δ 12.97, 9.01, 7.69, 7.51, 7.34, 7.14, 3.87, 3.58, 3.23, 3.09. HRMS (ESI) calculated for $C_{54}H_{59}BF_3N_6O_8S^+$ $(M+H)^+$: 1019.4155, found 1019.4146 (Δ 0.9 ppm). Analytical HPLC-MS retention time with a a10-90% H_2O:ACN (0.05% TFA), 20 min gradient, 1 mL/min: 14.8 min. Preparative HPLC with a a10-90% H_2O:ACN (0.05% TFA) 20 min gradient: 13.3-13.7 min.

HPLC-MS: H_2O:ACN (0.05% TFA), 20 min gradient, 1 mL/min flow, det. 215 nm 280 nm:

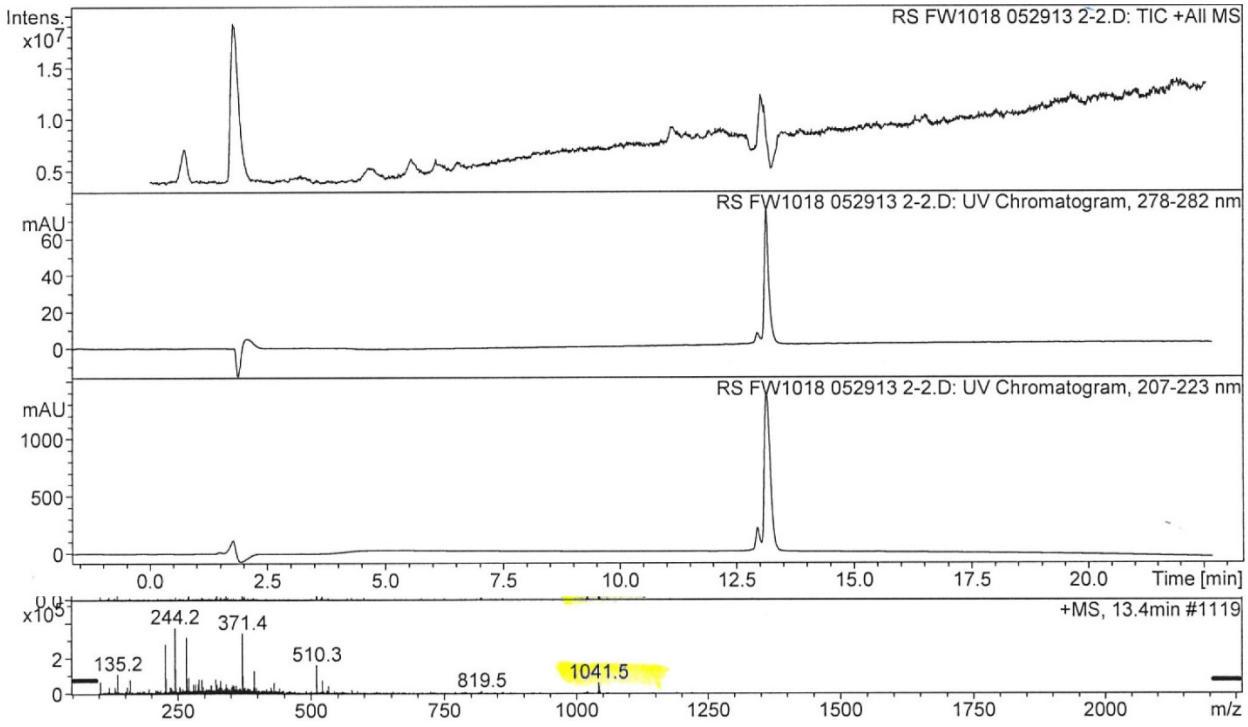

HRMS-ESI$^+$:

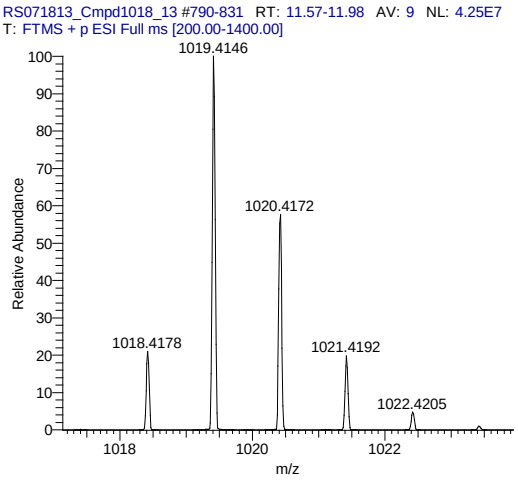

1.7 Synthesis of biotinylated-pinacol protected dioxaborolane probe, 1. A 1.5 mL Agilent screw top micro sampling vial (Agilent 5184-3550) was charged with boronate **v** (12.1 mg, 11.88 µmol), heptacyanine dye **i** (12 mg, 14 µmol), N-Hydroxybenzotriazole (14 mg, 91 µmol), DMF (800 µL), and pyridine (80 µL). The reaction was initiated with the addition of EDC (150 mg), placed in a Branson 2510 sonicator for 10 min, and left at room temperature for 2 hours. N-hydroxy succinimide (14 mg) was added and left at room temperature for 2 hours. The reaction was chromatographed directly on a preparative reverse phase HPLC. Fractions containing **1** were lyophilized as H_2O:ACN mixtures to give **1** as a solid green compound (2.4 mg, 1.2 µmols, 13% yield) that is aliquoted and stored at -78 °C.

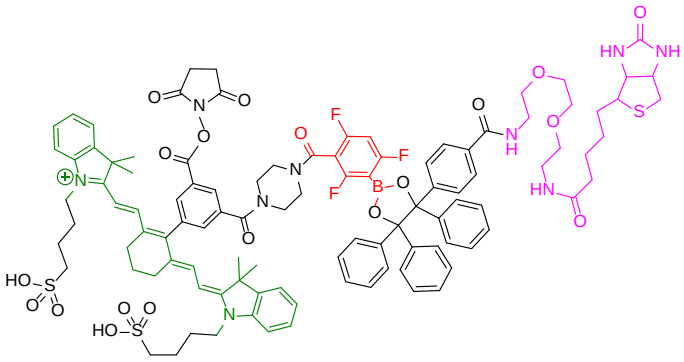

1

Chemical Formula: $C_{104}H_{112}BF_3N_9O_{19}S_3^+$
Exact Mass: 1954.7276
Molecular Weight: 1956.0516

m/z: 1955.7315 (100.0%), 1954.7282 (88.9%), 1956.7349 (55.7%), 1954.7352 (24.8%), 1953.7318 (22.1%), 1957.7382 (20.5%), 1955.7385 (13.8%), 1957.7273 (13.6%), 1956.7240 (12.1%), 1958.7307 (7.6%), 1958.7416 (5.6%), 1955.7276 (5.1%), 1956.7419 (5.1%), 1957.7358 (3.9%), 1956.7324 (3.5%),

^{1}H NMR (DMSO-d6, 500 MHz, 21 °C): δ 12.97, 9.01, 7.69, 7.51, 7.34, 7.14, 3.87, 3.58, 3.23, 3.09. HRMS (ESI) calculated for $C_{104}H_{112}BF_3N_9O_{19}S^+$ $(M+H)^+$: 1954.7276, calculated for $C_{104}H_{113}BF_3N_9O_{19}S^{+2}$ $(M+H)^{2+}$: 977.8674, found 977.8708 (Δ 3.5 ppm). Analytical HPLC-MS retention time using a a10-90% H_2O:ACN (0.05% TFA), 20 min gradient, 1 mL/min: 17.8 min. Preparative HPLC with a a10-90% H_2O:ACN (0.05% TFA) 20 min gradient: 19.0-20.0 min.

HPLC-MS: H_2O:ACN (0.05% TFA), 20 min gradient, 1 mL/min flow, det. 280, 215, 780, 650 nm:

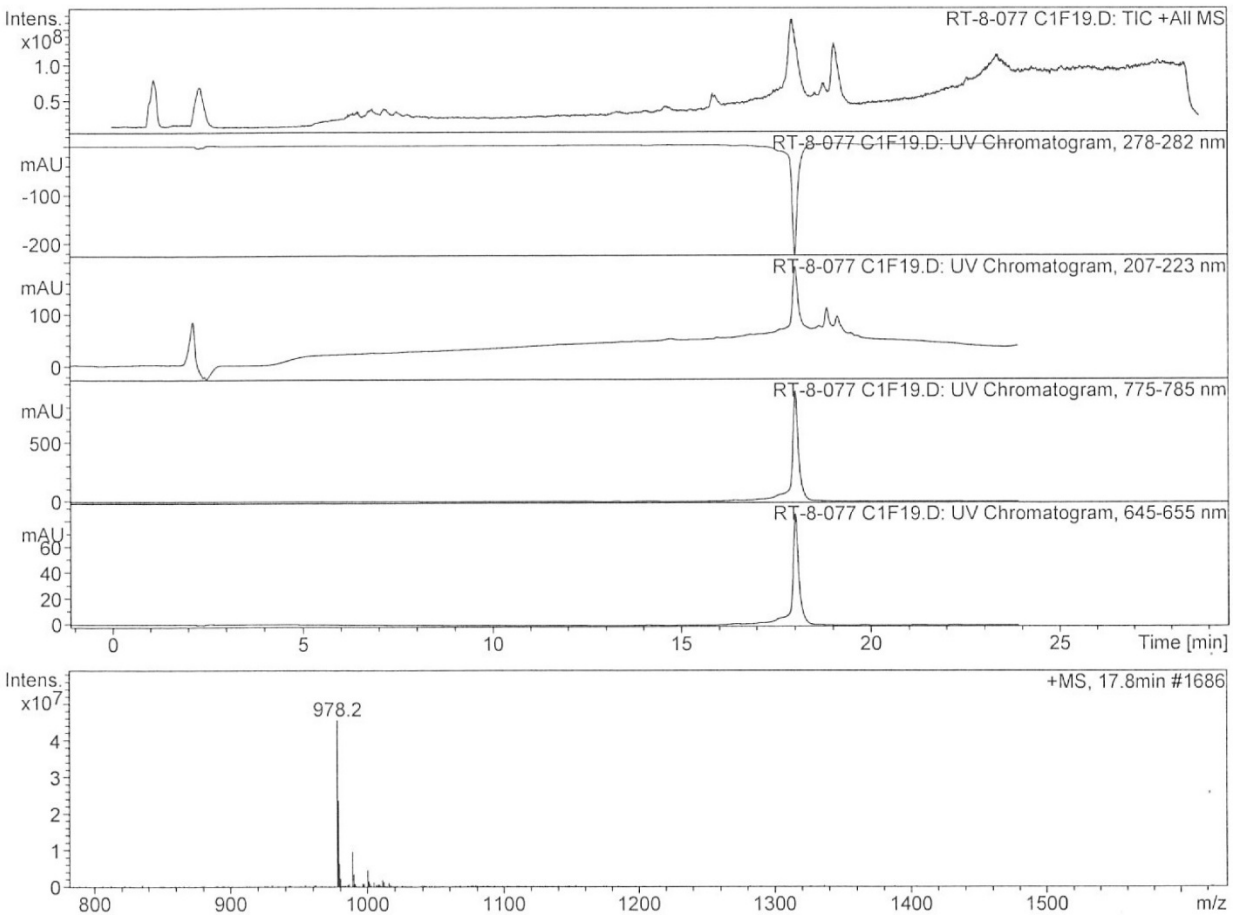

HRMS-ESI$^+$:

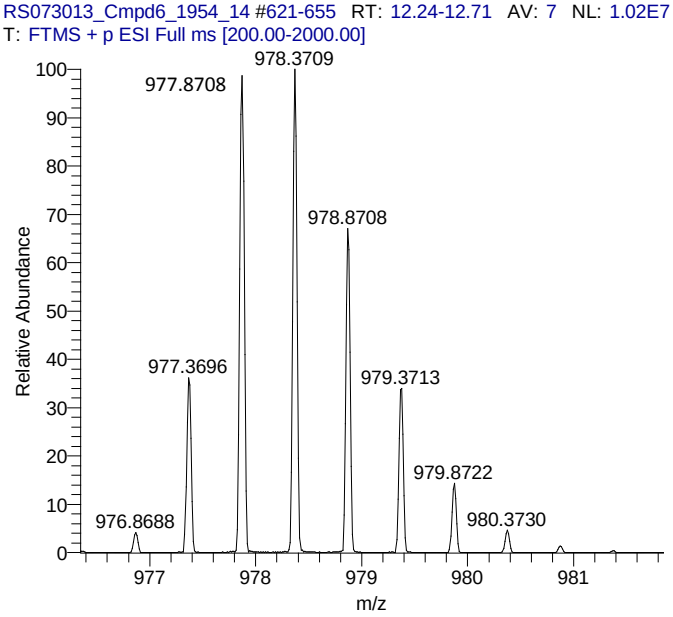

2. Small Molecule Fluoride Reactivity and Streptavidin Capture

2.1 Proof of aqueous trifluoroborate formation. Treatment of **1** with aqueous fluoride (pH 3) converts **1** into a biotinylated pinacol and a fluorescent trifluoroborate **2** (Scheme S3, Figure S1). The fluoride ion rate-dependence and lack of observed mono and/or difluoroborate intermediates (Figure S2) suggests that pinacol displacement is the rate-limiting step. Binding to streptavidin-agarose sequesters the biotinylated pinacol moiety either before or after fluoridation.

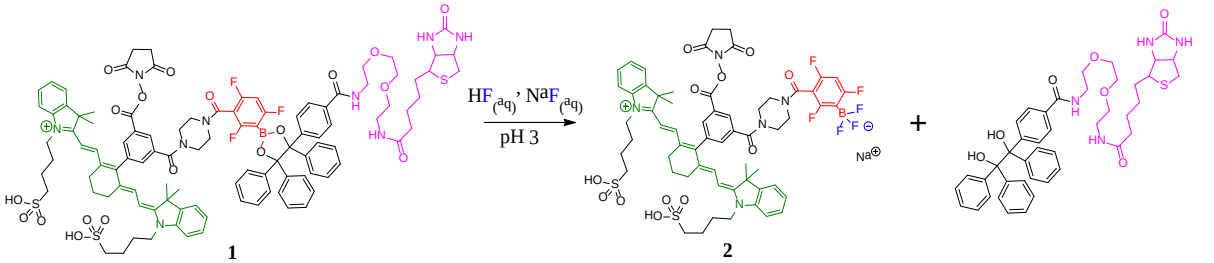

Scheme S3. Fluoride treatment of **1** frees biotinylated pinacol from the [^{18}F]-PET/NIRF probe (**2**) via trifluoroborate formation.

1 and the fluoridated probe **2** can covalently attach to a primary or secondary amine via the reactive NHS ester. The resulting fluoride bearing biomolecule is visible by both PET (when reacted with [^{18}F]-fluoride) and NIRF.

2.2 Synthesis of Mal-1. N-(2-Aminoethyl) maleimide trifluoroacetate salt was reacted with **1** under aqueous conditions to give Mal-**1**, a compound that does not undergo NHS-ester hydrolysis. N-(2-Aminoethyl) maleimide trifluoroacetate salt (1 mg, 3.9 µmols) and 1.8 µL NMM were added to 186 µL of 2.1 mM **1** in DMSO (390 nmol) in a 1.5 mL micro sampling vial. The reaction was incubated for 1 hour and chromatographed by preparative, reverse phase HPLC. Fractions containing Mal-**1** were lyophilized to give Mal-**1** (green compound).

HRMS (ESI) calculated for $C_{106}H_{116}BF_3N_{10}O_{18}S_3^+$ $(M+H)^+$: 1,978.7520, calculated for $C_{106}H_{116}BF_3N_{10}O_{18}S_3^{2+}$ $(M+H)^{2+}$: 990.3833, found 990.3863 (Δ 3.0 ppm). Analytical HPLC-MS retention time using a a10-90% H_2O:ACN (0.05% TFA), 20 min gradient, 1 mL/min: 18.5 min (See Figure S1 for HPLC-MS traces).

HRMS-ESI$^+$:

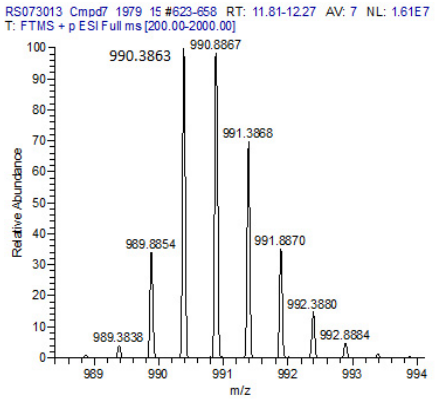

2.2.1 Fluoridation of Mal-1. A 1 µL, 145 µM solution of Mal-**1** (Figure S1) in 50:50 ACN:H_2O was added to a 60 µL microcentrifuge tube containing 19 µL of 29 mM HF in 50:50 ACN:H_2O (pH 3) to give a final, 20 µL solution containing 7.3 µM Mal-**1** and 270 mM HF. This reaction was incubated at room temperature for 1 hour and analyzed by reverse phase HPLC. Absorbance spectra of Mal-**1**, observed at 780 nm, demonstrates quantitative conversion to the trifluoroborate (Mal-**2**, Figure S1). Mal-**2** HPLC-MS retention time is 15.2 min using a a10-90% ACN:H_2O (0.05% TFA), 20 min gradient, and 1 mL/min flow. The released pinacol bearing biotin is also observed in 215 nm HPLC absorbance spectra (Figure S1).

2.2.2 Concentration dependent fluoride triggered trifluoroborate release. Four micro centrifuge vials were loaded with 19 µL of 0.285, 2.85, 28.5, or 285 mM HF solution (50:50 ACN:H_2O, pH 3). 1 µL of 145 µM Mal-**1** in 50:50 ACN:H_2O was added to each vial to give 20 µL solutions containing 7.3 µM Mal-**1** and 0.27, 2.7, 27, or 270 mM HF. The reactions were incubated at room temperature for 2 hours and analyzed by reverse phase HPLC. HPLC absorbance (detected at 780 nm) shows trifluoroborate formation is highly dependent on fluoride concentration (Figure S2).

Fluoridation occurs within 2 hours (approximately one [^{18}F] half-life) at HF concentrations >27 mM and very slowly at concentrations <2.7 mM. Interestingly, at 27 mM HF there is a distribution of NIRF signal between only two species: Mal-**1** and its trifluoroborate, Mal-**2**. The use of smaller fluoride concentrations is preferred for high-specific activity radiosyntheses. The lack of mono- or di-fluoroborate products allow us to hypothesize: 1) That pinacol displacement is the rate-limiting step and 2) At pH 3, the fluoride ion is greater than 10,000 times more reactive then the H_2O nucleophile at 27.8 M (50:50 ACN:H_2O).

2.2.3 Streptavidin-specific iron-oxide binding of 1/Mal-1. To show that the biotin handle on **1** or Mal-**1** can be sequestered using streptavidin-solid support, five 250 μL pulled point glass inserts (Agilent, 5183-2085) were charged with 100 μL of 1x DPBS (10 mM PBS, pH 7.4, Life Technologies, 14190-136). Four of these inserts serve as controls (Inserts 1, 2, 4, and 5). To Inserts 1, 3, and 4, 1 μL of 145 μM solution of fluorescent Mal-**1** (145 pmol) was added. 10 μL of 100 mM D-biotin in DMSO (1 μmol) was added to Insert 4 to give a solution with a 9.1 mM final biotin concentration. In another control, 1 μL of 145 μM Mal-**1** was mixed with 20 μL of 30 mM HF solution in Insert 5 for 20 min (1 μmol) and then brought to pH 7.4 with 100 μL of 1x DPBS. To capture Mal-**1**, 20 μL of streptavidin-dynabeads® M-270 iron oxide (IO, Invitrogen 65305) were added to Inserts 3, 4, and 5. Solutions were incubated for 5 min before inserts were placed on a magnetic rack, which caused pelleting of streptavidin-IO. Magnetized inserts were imaged on CRI Maestro full field fluorescence imaging device. Filters used for Cy7 fluorescence imaging are excitation/emission = 730(42)/800LP nm, respectively.

The fluorescence contained in Insert 3 is entirely localized to the pellet, indicating binding between the biotin moiety on Mal-**1** to streptavidin-IO particles (Figure S3). All other inserts serve as controls. Pelleted fluorescence is not observed in Insert 1. Auto-fluorescence is not observed in DPBS (Insert 2). The pelleted fluorescence is not observed in Insert 4 because streptavidin binding sites are blocked with excess free biotin. Fluorescence pelleting is not observed in Insert 5, because Mal-**2** lacks a biotin handle for binding to streptavidin-IO particles.

2.2.4 Fluoride triggered elution of trifluoroborates from streptavidin-agarose bound complexes of Mal-1. Streptavidin-IO disintegrates in acidic fluoride solutions and a different solid-support was necessary to test HF triggered elution of Mal-**2**. The following experiment was performed to prove that the biotin handle on Mal-**1** is sequestered by streptavidin-agarose before and after HF treatment. A Luer-lock-fitted Millipore Millex-GV, 0.22 μm, PVDF, 4 mm filter was charged with 10 μL streptavidin-agarose (Solulink, N-1000-005) and 1 μL of 145 μM Mal-**1**. Conversion of Mal-**1** to Mal-**2** was initiated with the addition of 10 μL of 30 mM HF + 1.4 μL of 1.5 M HCl (6.5 μM Mal-**1**, 13.4 mM HF, and 93 mM HCl, total volume 22.4 μL). HCl (pH 3) was necessary to compensate for the buffering capacity of streptavidin-agarose storage solution without increasing fluoride ion carrier concentration. The fluoridation reaction was incubated for 40 min at room temperature and the reaction was quenched with 50 μL of 8x DPBS + 20% EtOH. A syringe was used to flush the solution-phase into a mass spectrometry vial for analysis by reverse phase HPLC. HPLC analysis of the eluent shows a 780 nm absorbent peak with a retention time that corresponds to only the trifluoroborate, Mal-**2**. The eluted trifluoroborate (Mal-**2**) absorbance at 780 nm (Figure S4b) is only 5-10% of the starting 780 nm

absorbance (Figure S4a), indicating that the majority of the biotinylated Mal-**1** remains bound to the streptavidin-agarose. No starting material (Mal-**1**) was detected in the eluent (Figure S4b), showing the biotin on Mal-**1** remains bound to streptavidin-agarose and prevents elution of Mal-**1** with the desired trifluoroborate, Mal-**2**. These experiments describe a system that is analogous to ^{99m}Tc radiotracer generation via a ^{99}Mo generator. We demonstrate the construction of a solid-support that can be flushed with reagents to elute the desired, pure radiotracer.

3. Antibody Labeling, Generator Construction, and Fluoride Release

3.1 mAb/Cetuximab labeling with the boronate/NIRF probe, 1. **1** (1 μL, 2,100 pmols, 2.1 mM in DMSO) was added to 62.5 μL of a 20 μM mAb solution (1,250 pmols, EpCAM/TROP1 mAb (Clone 158206, R&D systems, MAB9601)) or Erbitux® (Cetuximab, ImClone). Amide bond formation was initiated with 2.6 μL of 910 mM NMM with total volume of 66.1 μL containing 32 μM **1**, 19 μM mAb, and 36 mM NMM for 1 hour. Absorbance based quantification gave 1-2 molecules of Cy7 per mAb. mAb-**1**/Cetuximab-**1** synthesis was verified by SEC HPLC on a Shodex 802.5, 400 Å, 300 cm x 8.0 mm silica hydrophilic polymer column (F6989000) using an isocratic solution of 250 mM PBS (pH 7.5) and a flow rate of 1 mL/min. mAb-**1**/Cetuximab-**1** elutes between 5-7 min. mAb-**1**/Cetuximab-**1** labeling was also verified by PAGE (Figure 2). mAb-**1**/Cetuximab-**1** is visible by Cy7 fluorescence (CRI Maestro^{TM} full field fluorescence imager; excitation/emission of 730(42)/800LP nm, respectively).

3.1.1 Size exclusion chromatography of mAb and mAb-1. mAb-**1** labelling was verified by SEC HPLC with a 802.5, 400 Å, 300 cm x 8.0 mm silica hydrophilic polymer column (Shodex, F6989000) using an isocratic solution of 100 mM PBS (pH 7.5) and a flow rate of 1 mL/min to elute mAb-1. On an Agilent 1100 HPLC, mAb-**1** elutes at ~8 min (Figure S5). Note that the use of this SEC HPLC column on a Beckman Coulter System Gold HPLC in later, radioactive experiments, gives earlier mAb elution times, between 5-7 min.

3.1.2 Polyacrylamide gel electrophoretic (PAGE) analysis of mAb-1. mAb-**1** labeling was verified by polyacrylamide gel electrophoresis (PAGE). 6 μL mAb-**1** aliquots (>10 pmols) were added to 2 μL volumes of NuPAGE LDS (4x) sample buffer (Invitrogen, NP0008). Samples were loaded on a NuPAGE 4-12% Bis-Tris polyacrylamide gel (Invitrogen, NP0323) and run in 1xNuPAGE MOPS SDS running buffer (Invitrogen, NP0001) at 150 V for 45 min. A precision plus protein dual color standard MW ladder (Bio-Rad, 161-0374) was run alongside samples. mAb-**1** is visible by fluorescence

imaging on a CRI Maestro full field fluorescence imager with excitation/emission of 730(42)/800LP nm, respectively. All loaded protein (mAb and mAb-**1**) was imaged by coomassie staining (2.75 mM Brilliant Blue R in 3 M HOAc for 60 min and overnight destaining in 20:10:70 MeOH:HOAc:H_2O). The mAb has a molecular weight of 150 kD.

3.2 Solid-phase mAb-1/Cetuximab-1 [$^{18/19}$F]-generator construction. 19.5 μL of mAb-**1**/Cetuximab-**1** (372 pmols) was added to 30 μL streptavidin-agarose (Solulink, N-1000-005) and incubated for 5 min. The mixture was transferred to a Spin-X 0.22 μm cellulose acetate filter (Costar, 8161) or a micro-spin column (30 μm polyethylene filter, Thermo Scientific, 89879) and was centrifuged at 4,000 rcf for 1 min. The filtrate was discarded and streptavidin-agarose was resuspended in 500 μL of diH_2O. The streptavidin-agarose was washed 3X 500 μL diH_2O to completely remove unconjugated mAb and PBS buffer from mAb-**1**/Cetuximab-**1**.

3.2.1 mAb-1 capacity of streptavidin-agarose. To determine the mAb-**1**-biotin-binding capacity of the streptavidin-agarose, 1.9 μL mAb-**1** aliquots (37 pmols) were transferred to 9 tubes, 7 of which contained 0, 0.4, 0.8, 1.4, 2, 4, or 8 μL of streptavidin-agarose and 8, 7.6, 6.6, 6.2, 6, 4, or 0 μL of H_2O, respectively (final volume = 9.6 μL, 3.8 μM mAb). Two additional tubes were prepared with 1.9 μL mAb and 12 or 16 μL streptavidin-agarose (final volume = 13.9 and 17.9 μL, 2.6 and 2.1 μM mAb). mAb-**1** binding to streptavidin-agarose proceeded for 15 min before the contents of each tube was transferred to a Spin-X 0.22 μm, cellulose acetate filter (Costar, 8161). Filtrates were collected by centrifugation at 4,000 rcf for 1 min and analyzed by PAGE (Figure S6). The observed binding capacity of streptavidin-agarose is 14 ± 5 pmols of mAb-**1** per μL streptavidin-agarose.

3.2.2 (Control) Non-specific binding is not observed between streptavidin-agarose and unconjugated, unmodified mAb. To show that streptavidin-agarose does not non-specifically bind unlabeled mAb, 500 μg of lyophilized mAb was dissolved in 125 μL of 1x DPBS. 1.0 μL aliquots (20 pmols mAb) were transferred to 9 tubes containing 0, 1, 2, 4, 8, 12, 16, 24, or 32 μL of streptavidin-agarose and 32, 31, 30, 28, 24, 20, 16, 8 or 0 μL H_2O (final volume = 33 μL, 606 nM mAb). After 15 min at room temperature, the contents were transferred to Spin-X 0.22 μm cellulose acetate filters (Costar, 8161). Filtrates were collected by centrifugation and analyzed by PAGE (Figure S7).

3.2.3 (Control) Non-specific binding is not observed between streptavidin-agarose and mAb-2. To show that streptavidin-agarose has little affinity to mAb-**2**, a species that lacks the

biotin moiety, the NHS-ester of the trifluoroborate **2** was synthesized, purified by preparative HPLC, and reacted with mAb to give pure mAb-**2** (Figure S8). **1** was converted to its trifluoroborate by incubating **1** (18 μL, 37 nmols, 2.1 mM **1** in DMSO) with 18 μL of 1 M HF (18 μmols) for 60 min at room temperature. The entire reaction (36 μL) was loaded on a reverse phase HPLC and purified on a a10-90% H_2O:ACN (0.05% TFA), 20 min gradient, with a flow rate of 1 mL/min. Fractions between 16-17 min were collected, pooled, frozen under liquid N_2, and lyophilized overnight. Absorbance at 780 nm shows quantitative conversion of **1** to the NHS-ester trifluoroborate (**2**) (Figure S8).

The lyophilate of **2** was suspended in 10 μL 50:50 DMSO:ACN (1.3 mM **2**, determined by absorbance measurement at 780 nm (Thermo Scientific NanoDrop 2000c spectrophotometer)). NHS ester **2** (0.33 μL, 429 pmol) in 50:50 DMSO:H_2O was added to mAb (18 μL, 360 pmols, 20 μM). NHS labeling of mAb was performed with 23 μM of **2**, 19 μM of mAb, and 195 mM of NMM. The reaction was incubated for 30 min before 1.9 μL aliquots (36.7 pmols mAb) were transferred to 6 solutions containing 4, 8, 12, 16, 24, or 32 μL streptavidin-agarose. The mixture was incubated for 15 min and contents were transferred to a Spin-X 0.22 μm cellulose acetate filter (Costar, 8161). Filtrates were collected by centrifugation and analyzed by PAGE (Figure S9).

3.3 Fluoride concentration dependent mAb-2/Cetuximab-2 elution from streptavidin-agarose. To demonstrate that mAb-**1**/Cetuximab-**1**-bound streptavidin-agarose reacts with aqueous fluoride to generate mAb-**2**/Cetuximab-**2** and trigger mAb-**2** (Figure 2b)/Cetuximab-**2** removal from solid-phase, mAb-**1** (372 pmols mAb, 19.5 μL) was added to 30 μL of streptavidin-agarose for 5 min before the entire reaction was transferred onto a Spin-X 0.22 μm cellulose acetate filter (Costar, 8161). This filter was centrifuged at 4,000 rcf for 1 min and the filtrate was discarded. The resulting streptavidin-agarose was resuspended in 800 μL H_2O and then centrifuged at 4,000 rcf for 1 min. The streptavidin-agarose was washed 3X to remove NMM and DPBS from mAb-**1**. mAb-**1** bound to streptavidin-agarose was resuspended in 70 μL diH_2O and transferred in 5 μL aliquots to 15x 30 μm polyethylene filtered micro-spin columns (Thermo Scientific, 89879). 10 μL volumes of a HF (pH 3) dilution series was added to the micro-spin columns to give vials with a final volume of 15 μL, concentrations of 0.40, 1.2, 3.6, and 11 mM fluoride, and 1.7 μM mAb-**1** (26.5 pmols). Fluoridation was incubated for 1 hour and reactions were quenched with 10 μL of 1 M PBS (pH 7.4). Filtrates were collected by centrifugation and analyzed by PAGE.

4. Radiolabeling and Specific Activity

4.1 Radioactive [^{18}F]-fluoride ion concentration. 70 μL of 29.1 mCi (t = 0 min) [^{18}F]-sodium fluoride solution (PETNET) was transferred to a class A, borosilicate top microsampling vial (Agilent, 5184-3550) fitted with a rubber septa sealed screw cap (Agilent, 5182-0717). N_2 was passed over the radioactive liquid at room temperature through an 18G1/2 needle and N_2 carrying radioactive H_2O vapor was vented through an 18G needle outlet, 75 feet of Tygon S-50-HL tubing, and forced through 45 lbs of activated carbon with an 8" inline fan rated at 108 Watts and 483 cubic feet per min. Complete evaporation took place in 14 min with a 10 psi flow. The resulting vial contained a decay corrected activity of 28.44 mCi (26.0 mCi measured at t = 14 min), or 97.7% starting activity. 10 μL diH_2O was added to the vial to resuspend the [^{18}F]-fluoride concentrate. A 6 μL, 12.67 mCi decay corrected volume was recovered and transferred to polypropylene tubes for mAb-**1** labeling (7.44 mCi measured at t = 83 min). This recovered volume corresponds to 43.5% starting activity.

4.2 Solid-phase, [^{18}F]-fluoride radiolabeling of mAb-1/Cetuximab-1 and [^{18}F]-mAb-2/Cetuximab-2 elution. Cocktails of ^{18}F-^{19}F were made by adding 29 mCi to 60 nmol of ^{19}F to give an SA of about 0.5 Ci/μmol. Dry, mAb-**1**/Cetuximab-**1**-bound streptavidin-agarose (1,200 pmols mAb) in 30 μm polyethylene filtered micro-spin columns were resuspended in 4 μL of a 29.3 mCi [^{18}F]-fluoride solution (PETNET, time of reaction (TOR) = 0 min), containing 1.5 μL of 1 M HCl, and 1.5 μL of 37 mM [^{19}F]-carrier hydrogen fluoride (pH 2-3, final volume 15 μL, HCl is required to quench buffer that is introduced by the mAb and Solulink streptavidin-agarose). Room temperature nitrogen flow was passed over the streptavidin-agarose as fluoridation proceeded for 69 min (TOR = 69 min) before 50 μL of 250 mM PBS (pH 6.5) was added to neutralize. The micro-spin column was centrifuged to elute radiolabeled [^{18}F]-mAb-**2**/Cetuximab-**2** and was chromatographed by isocratic SEC HPLC using 250 mM PBS (pH 6.5, [^{18}F]-mAb-**2**) or 25 mM PBS (pH 6.5) and 200 mM NaCl as eluents (Cetuximab-**2**). [^{18}F]-mAb-**2**/Cetuximab-**2** elutes between 5-7 min, in a fraction containing both [^{18}F]-activity and Cy7 fluorescence. [^{18}F]-mAb-**2**/Cetuximab-**2** is injected into mice immediately following elution.

4.3 Calculation of specific activity. The correlation between antibody mass and 215 nm absorbance on SEC HPLC was determined by injecting 1, 2, 3, 4, and 5 μL known-quantity solutions of Cetuximab at (2 mg/mL, GMP grade for patient injection) in ~ 50 μL volumes (1x PBS) through a 802.5, 400 Å, 300 cm x 8.0 mm silica hydrophilic polymer column (Shodex, F6989000) at a 1 mL/min flow rate with a running buffer of 25 mM PBS and pH 6.5 200 mM NaCl (Cetuximab), or 200 mM PBS (mAb-**1**)

and a 1 mL injection loop. This ladder is used to correlate 215 nm absorbance on the HPLC detector with injected mAb mass. Fractions corresponding to antibody elution at 6-7 min were collected and reinjected to estimate recovery. This analysis assumes that the 215 nm contribution by the PET/NIRF probe is negligible. On average 60% of the antibody was recovered between 6-7 min fractions.

HPLC radioisotope detector voltage also needed to be correlated with radioactivity. This was determined by eluting radioactive ^{18}F-Cetuximab-**2** or mAb-**2** by SEC HPLC. The antibody fraction (6-7 min) was collected and measured on a Capintec CRL-SSt v3.08 well counter. If less than 20 µCi was isolated these samples were placed on a Wallac Wizard 3" or Beckman scintillation counter alongside a dilution series of ^{18}F-ion where activity had been measured in a Capintec CRL-SSt v3.08 well counter. The calculated activity was adjusted for its 60% loss on the SEC HPLC column (calculated above). 215 nm absorbance was monitored at the same time as radioisotope detector voltage in a sample of interest. 215 nm absorbance could be correlated with mass using the ladder generated with known-quantity solutions. Radioisotope detector voltage could be correlated with activity by scintillation counter. These correlations allow us to estimate specific activity.

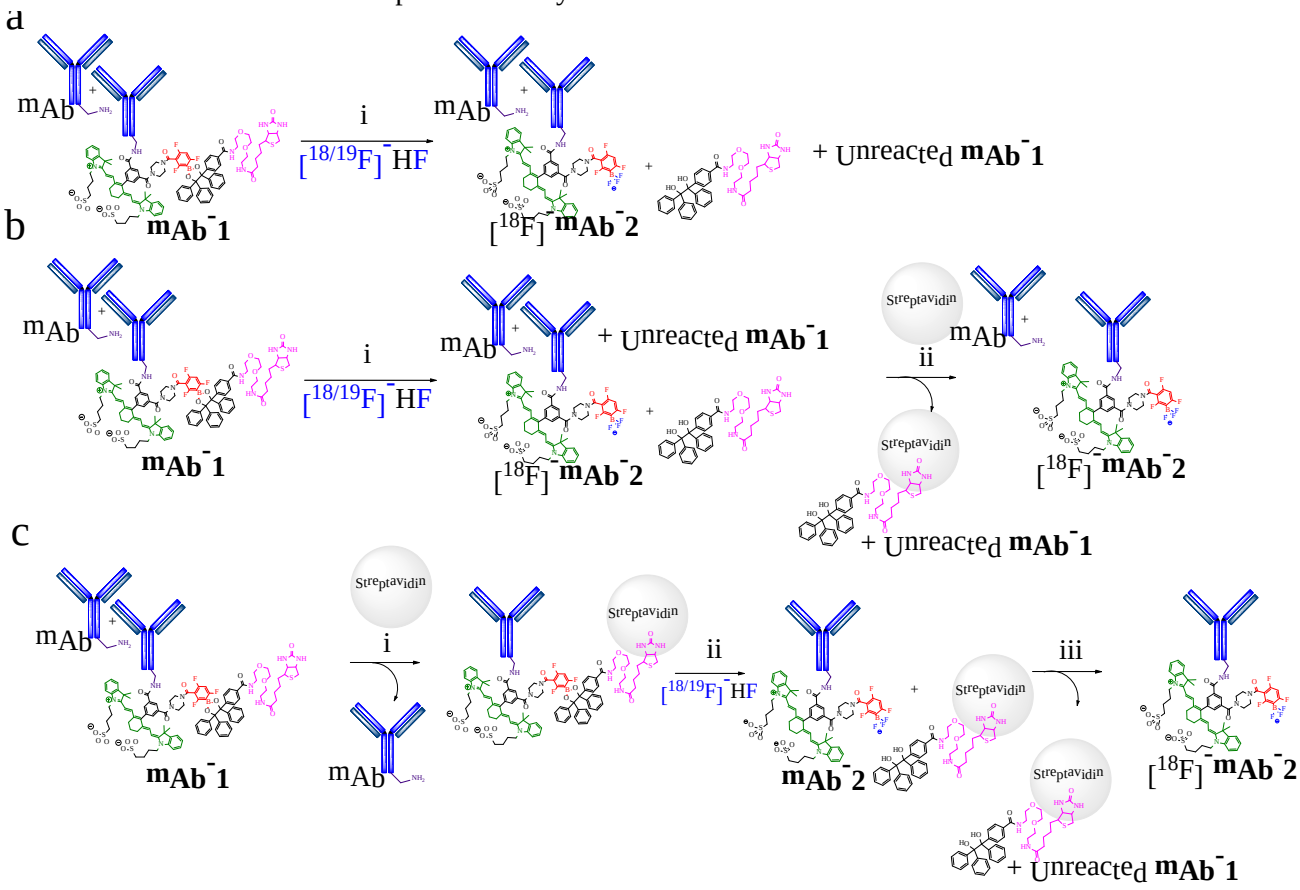

Scheme S4. Three different syntheses of [^{18}F]-mAb-**2** to monitor the effect of streptavidin-agarose on specific activity.

(a) Direct, solution-phase mAb-**1** [^{18}F]-fluoridation. (i) A solution of mAb-**1** is reacted with [^{18}F]-fluoride. Streptavidin-agarose is not employed, and resulting [^{18}F]-mAb-**2** is contaminated with mAb-**1** and unreacted mAb. (b) Streptavidin-agarose workup of a solution-phase [^{18}F]-mAb-**2** synthesis. (i) mAb-**1** is reacted with [^{18}F]-fluoride. (ii) the products are incubated with streptavidin-agarose and centrifuged through a filter, removing mAb-**1** from a solution of [^{18}F]-mAb-**2** that is contaminated with unreacted mAb. (c) [^{18}F]-fluoride triggered mAb-**2** elution from streptavidin-agarose. The synthesis of [^{18}F]-mAb-**2** is performed as reported in Scheme S1. The resulting [^{18}F]-mAb-**2** is pure and lacks mAb-**1** and unreacted mAb.

4.4. Direct, solution-phase mAb-1 [^{18}F]-fluoridation (Scheme S4a). Reagents were added to 2.5 μL mAb-**1** (375 pmols) in the following order: 2 μL of 2.5 mCi [^{18}F]-sodium fluoride (1.2 μCi/μL specific concentration at time of reaction (TOR = -6 min)) and 0.5 μL of 37 mM [^{19}F]-fluoride carrier. Fluoridation was started with 1.0 μL of 1 M HCl to adjust pH to 3 (TOR = 0 min). The resulting 6.0 μL [^{18}F]-fluoridation contained 62 μM of mAb (375 pmols), HCl (1 nmol), 2.5 mCi [^{18}F]-sodium fluoride, and 3.2 mM carrier [^{19}F]-fluoride (19.6 nmols). Fluoridation was incubated for 130 min (TOR = 130 min) at room temperature, quenched with 50 μL of 250 mM PBS (pH 6.5), and loaded directly on a Beckman Coulter System Gold HPLC equipped with a SEC 802.5, 400 Å, 300 cm x 8.0 mm silica hydrophilic polymer column (Shodex, F6989000). Absorbance readings were measured on a System Gold 166 detector at 215 nm. Radioactivity was measured on a Beckman 170 radioisotope detector. [^{18}F]-mAb-**2** was eluted using isocratic 250 mM PBS (pH 6.5) with a flow rate of 1 mL/min. The [^{18}F]-mAb-**2** elutes at 5-7 min, possesses a 215 nm peak absorbance of 83 mAU, and is well separated from [^{18}F]-fluoride, which elutes at 13 min (Figure S10). 1 mL fractions were manually collected every min (1-20 min). Long wavelength HPLC absorbance and fluorescence detection was not available so fractions were collected and were imaged on a CRI Maestro full field fluorescence imaging device after quantitative [^{18}F]-fluoride decay (24 hour later). Cy7 was imaged by fluorescence with a 5 sec exposure and excitation/emission = 730(42)/800LP nm, respectively. [^{18}F]-activity was quantitated on a Beckman Scintillation counter at (t = 381 min). The mAb-**2** fraction (6 min) has a cpm reading of 67,904.

4.5 Streptavidin-agarose workup of a solution-phase [^{18}F]-mAb-2 synthesis (Scheme S4b). A 2.5 μL mAb-**1** aliquot (150 pmols) was reacted with 2 μL of 2.5 mCi [^{18}F]-sodium fluoride (TOR = -6 min), 0.53 μL of 37 mM carrier [^{19}F]-fluoride, and 1.0 μL of 1 M HCl (TOR = 0 min) as described previously. Fluoridation was incubated for 165 min at room temperature and reactions were quenched with 50 μL of 250 mM PBS (pH 6.5). 40 μL of streptavidin-agarose was added at 165 min and

transferred to a Pierce micro-spin column containing a 30 μm polyethylene filter. Biotin binding was incubated for 5 min and reactions were centrifuged at 4,000 rcf for 1 min. [^{18}F]-mAb-**2** elutes at 5-7 min, and possesses a 215 nm peak absorbance of 162 mAU when chromatographed by SEC HPLC. The scintillation quantified [^{18}F]-activity of the mAb-**2** fraction (6 min) is 288,000 cpm (Figure S11).

4.6 [^{18}F]-fluoride triggered mAb-2 elution from streptavidin-agarose (Scheme S4c).

A 18.9 μM solution of mAb-**1** (1,250 pmols, 66 μL) was mixed with 150 μL of streptavidin-agarose. Biotin binding was incubated for 5 min and transferred as 2x 105 μL aliquots to two 30 μm polyethylene filtered micro-spin columns. The spin columns were centrifuged at 4,000 rcf for 1 min and the filtrates were discarded. Spin columns were mixed and washed with 2X 200 μL diH_2O. The mAb-**1** bound streptavidin-agarose was resuspended in 15 μL of 52.3 mCi [^{18}F]-sodium fluoride (0.838 μCi/μL specific concentration (t = 0 min)), 0.45 μL of 1 M HCl, and 0.62 μL of 100 mM carrier [^{19}F]-HF (pH 3, 3.9 mM fluoride (^{19}F + ^{18}F), 63 pmols mAb, final volume = 16.02 μL). Fluoridation proceeded for 23 min at room temperature and 50 μL of 250 mM PBS (pH 6.5) was added to neutralize the reaction and stop fluoridation (t = 23 min). After PBS addition, micro-spin columns were centrifuged immediately at 4,000 rcf for 1 min. The filtrate was chromatographed by SEC HPLC (as described previously). Due to the reduced quantity of [^{18}F]-mAb-**2**, a 215 nm absorbance peak corresponding to [^{18}F]-mAb-**2** was difficult to observe. To conservatively estimate the enhancement of SA, the largest 215 nm absorbance peak, 4.3 min, was chosen to represent [^{18}F]-mAb-**2**. This peak possesses a 215 nm peak absorbance of 10 mAU in a fraction containing both [^{18}F]-activity and cyanine fluorescence (Figure S12). The scintillation [^{18}F]-activity of the mAb-**2** fraction is 88,976 cpm.

4.6.1 (Control) Attempted [^{18}F]-fluoridation of unmodified mAb. Unconjugated mAb was mixed with 5 μL of 2.50 mCi [^{18}F]-sodium fluoride (TOR = -6 min), carrier [^{19}F]-fluoride, and HCl. This reaction was incubated for 200 min at room temperature. The mixture was neutralized with 50 μL of 250 mM PBS (pH 6.5) and chromatographed by SEC HPLC. Non-specific binding was not observed between unmodified mAb and [^{18}F]-fluoride (Figure S13). The mAb elutes at 6 min, and possesses a 215 nm peak absorbance of 50 mAU when chromatographed by SEC HPLC. A radioisotope peak is not observed.

4.7 Estimate of specific activity (SA) enhancement due to streptavidin-agarose.

Streptavidin-agarose increases the SA of [^{18}F]-mAb-**2** radiosynthesis. The streptavidin-agarose functions by removing the unconjugated mAb and retaining unconverted mAb-**1** on the solid-phase, away from the solution-phase [^{18}F]-mAb-**2** (Scheme S4c). A SA enhancement is clearly observed in Figures S10-S12.

These SA increases can be further optimized by varying the [^{18}F]-starting activity, amount of [^{18}F] reacted with mAb-**1**, the presence of carrier fluoride, among many other variables. In these radiolabeling experiments, the SA enhancement associated with the use of streptavidin-agarose was calculated by comparing the ratio of scintillated activity over the 215 nm mAb absorbance in the different preparations (Figures S10-S12). These ratios were normalized to the preparation of [^{18}F]-mAb-**2**, where streptavidin-agarose was not employed (Scheme S4a). There is a 2.2-fold increase in SA when streptavidin-agarose is used to work up an aqueous synthesis of [^{18}F]-mAb-**2** (Scheme S4a vs. Scheme S4b and Figure S10 vs. Figure S11). There is a 13-fold increase in SA when [^{18}F]-mAb-**2** is eluted from streptavidin-agarose that contains mAb-**1** (Scheme S4a vs. Scheme S4c, and Figure S10 vs. Figure S12, Figure S14).

5. *In Vitro* Imaging

5.1 *In vitro* reduction of mAb-2. To demonstrate that fluoridation does not disrupt mAb-**2**-EpCAM antigen binding, mAb-**2** was deliberately reduced into fragments as a control to eliminate antigen binding. 1.5 μL aliquots of 19 μM mAb-**2** was added to 1.5 μL of 1 M freshly prepared dithiothreitol (DTT), β-mercaptoethanol (BME), or 3,3',3"-Phosphanetriyltripropanoic acid (TCEP). Samples with reductants were incubated for 2 hours at room temperature or 95 ˚C and analyzed by PAGE. TCEP treatment at room temperature or BME treatment at 95 °C were the best conditions for reducing mAb into component heavy and light chains without disrupting the Cy7 fluoresence (Figure S15). In fluorescence microscopy experiments, 175 pmols of mAb-**2** was treated with up to 500 mM TCEP in a 38 μL volume at room temperature. This reaction was diluted with 20 μL of 100 μM PBS (pH 6.5) (used in Figure 4c).

5.2 *In vitro* cell imaging with mAb-2. PC3 cells in DMEM (Corning, 10-014-CV) and A549 cells in RPMI 1640 (Gibco, 11875) were grown in 10% FBS (Atlanta Biological, S11150) + 1X penicillin-streptomycin (Fisher Sci., SV30010) growth media on poly-D-Lysine coated glass bottom culture dishes (MatTek, P35G-0-14-C). mAb-**2**/mAb/mAb-**2** + TCEP labeling was done in growth medium with incubation times listed in Figure 4. Unbound mAb-**2**/mAb/mAb-**2** + TCEP was removed by washing 2X 2 mL of growth medium and 2X 2 mL 1x Hank's balanced salt solution (HBSS, Life Technologies, 14065-056) + 2 g/L glucose + 20 mM HEPES (pH 7.4). Fluorescent images were taken on a Zeiss Axiovert 200M inverted microscope controlled by SlideBook software. Dyes/FPs were imaged with the following settings: DIO excitation/emission of 495(10)/535(25) nm, respectively. DsRed2 excitation/emission of 540(25)/595(50) nm, respectively. E2-Crimson excitation/emission of 628(40)/680(30) nm, respectively. Cy7 excitation/emission of 710(40)/785(62) nm, respectively.

6. *In Vivo* Imaging

6.1 Animal Experiments. All procedures conducted in mice have been approved by UCSD (#S04011) and WCMC (#2014-0007 and #2014-0030) IACUC and are consistent with the recommendations of the AVMA and the NIH Guide for the Care and Use of Laboratory Animals.

6.2 *In vivo* fluorescent imaging of tumors and metastases using mAb-2. 1.5 million PC3 cells were mixed with Corning matrigel matrix (4 mg/ml final concentration) in a total volume of 40 µL. This 40 µL mixture was injected subcutaneously into the lateral, dorsal, lower left flank of athymic nude mice. Tumors were grown for 16 weeks (diameter = 0.5 cm). Mice were anesthetized with 2% isoflurane at a 2 L/min flow and mAb-**2** (90 µg, 600 pmols) was introduced through an i.v. tail vein injection. Isoflurane anesthetized mice on a heated pad were imaged at multiple time points using a CRI Maestro™ or a Bruker Xtreme™ *in vivo*, full field fluorescence imaging device. FP/dye was imaged with the following filters: DsRed2 excitation/emission of 530(52)/580LP nm, respectively, and liquid crystal = 590 nm. Cy7 was imaged using an excitation/emission of 730(42)/800LP nm and liquid crystal = 810 nm.

6.3 *In vivo* imaging of native and denatured mAb-2 in PC3 tumors at extended time points (24-72 hours). A 19.3 µM mAb-**1** solution was divided into two 31 µL aliquots in preparation for injection in two PC3 tumor-bearing mice. In the first, non-denatured aliquot, 3 µL of 1 M HF and 3 µL of 1 M HCl were added and the sample was incubated for 1 hour at room temperature. The second reaction, a control reaction, was mixed with 3 µL of 1 M HF, 3 µL of 1 M HOAc, and heated to 95 °C for 1 hour to denature mAb-**2** and remove EpCAM binding affinity. After 1 hour, the reactions were quenched with 15 µL of 1 M Tris (pH 8). The pH neutral injectates were diluted to 100 µL with diH_2O and resulting solutions were injected into mice i.v. through the tail vein. *In vivo* imaging of the first, non-denatured aliquot is shown in Figure S16i,a-e upper panels. The imaging of the second, high temperature-denatured control aliquot is shown in Figure S16ii,a-e lower panels.

Isoflurane anesthetized mice were imaged 24, 48, and 72 hours following injection using a CRI Maestro full field fluorescence imaging device. DsRed2 was imaged using excitation/emission = 530(52)/580 nm, respectively, and LCD = 590 nm. Cy7 was imaged using excitation/emission = 730(42)/800LP nm, respectively, LCD = 810 nm.

When viable mAb-**2** is administered i.v. in mice, (Figure S16ic,id) mAb-**2** fluorescence co-localizes with the fluorescence of the DsRed2 expressed in the primary tumor (Figure S16ib) is observed

at 24, 48, and 72 hours time points (only 72 hours is shown in Figure S16). When mAb-**2** is denatured with heat and HOAc, mAb-**2** accumulation at the primary tumor is not observed, but Cy7 fluorescence is still visible in clearance organs, such as the liver (Figure S16iic,iid). Figure S16b (DsRed2) and Figure S16c,d (Cy7) are adjusted the same for each fluorophore. This experiment shows that mAb-**2** accumulation at the primary tumor is due to antigen binding and not to non-specific tumor enhanced permeation and retention (EPR).

6.3.1 Confirmation of fluoridated Cetuximab-2 binding to EGFR expressed on A549 cells. Cetuximab (Erbitux) was substituted for mAb (EpCAM) because of its current clinical relevancy[45]. Instead of PC3 xenografts, an EGFR expressing orthotopic adenocarcinoma cell line (A549) was chosen for xenograft [^{18}F]-PET imaging studies[46]. To verify that fluoride treatment of Cetuximab-**1** (pH 3) does not compromise binding to EGFR expressed on A549 cells, solutions of Cetuximab-**1** (0.7 mg/mL) were incubated with 12-2,000 mM HF (pH 3) and 12-111 mM HCl. An nonfluorinated sample of Cetuximab-**1** was stored at pH 7.5 as a control. Reactions were incubated at 21 ˚C for 2 hours and neutralized with 40 µL of 1x DPBS. Cetuximab-**2** was purified by Melon Gel IgG spin purification (Thermo Scientific) and incubated with A549 cells for 1 hour. Streptavidin-agarose was not used to remove Cetuximab-**1** from mAb populations. Binding of Cetuximab-**1**/**2** to A549 cells was analyzed by flow cytometry (Gallios 1) using direct Cy7 fluorescence. Fluoride treatment of Cetuximab-**1** (pH 3) and DPBS neutralization does not inhibit recognition of EGFR the surface of A549 cells (Figure S17).

6.3.2 Confirming location of A549 primary tumor and metastasis into the lung. 2 million A549 cells expressing GFP, luciferase, and EGFR (required for Cetuximab binding) (35 µL) were mixed with 35 µL matrigel and injected into the chest wall/pleural cavity to a depth of 6 mm using a 25 G needle through the intercostal space on the left rib cage below the clavicle and just right of the left anterior axillary line of eight mice[47]. Tumor growth was monitored weekly by bioluminescence imaging on a Bruker Xtreme^{TM} full field fluorescence imaging device (Figure S18a). 50 µL of 3 mg/ml luciferin in PBS was injected intraperitoneal 5 minutes before imaging in mice that were anesthetized using 2% isofluorane. An exposure time of 1-10 seconds was used. After 38 days, mice were injected with 67 pmols (10 µg) of [^{18}F]-Cetuximab-**2** and mice were [^{18}F]-PET imaged on a Siemens Inveon PET/CT scanner (60-90 min) 1.5 or 4.5 hours (Figure 6b,c) after injection. Mice were sacrificed and tissue was harvested. Lung metastasis was confirmed by *in vivo* CT (Figure S18b), PET (Figure S18c), PET/CT (Figure S18d), macroscopic bright field inspection (Figure 6d, Figure S18e), fluorescent macroscopic-organ-imaging

(Figure 6e,f), and primary and lung tumor fluorescence detection in histology slides (Figure 6i,j). Primary tumor growth on the chest wall and lung tissue metastasis were observed in all mice.

6.4 *In vivo* PET/NIRF imaging and scintillation of primary and metastatic orthotopic lung A549 tumors using [^{18}F]-Cetuximab-2. Cetuximab-**1** was radiolabeled with [^{18}F]-fluoride and purified by SEC. [^{18}F]-Cetuximab-**2** elutes in 8-10 min and fractions were divided into 200 µL, 10 µg [^{18}F]-Cetuximab-**2** aliquots. [^{18}F]-Cetuximab-**2** was i.v. injected through the tail vein into eight mice 38 days after A549 cell inoculation. One mouse perished upon injection due to the advanced progression of the infiltrative cancer. Mice were anesthetized with 2% isoflurane and [^{18}F]-Cetuximab-**2** (25-100 µCi, 10 µg/mouse) was introduced through an i.v. tail vein injection. Mice were fixed on trays such that up to four mice could be imaged simultaneously along with a 200 mL flask containing ~40 ˚C water in a Siemen's Inveon PET/CT. A 10 min CT scan and a PET scan were acquired at 1.5 and 4.5 hours [^{18}F]-Cetuximab-**2** post-injection (PI). Three of the seven mice were imaged in a 1 hour long PET/CT scan, 1.5 hours PI, and were immediately sacrificed 2.5 hours PI. The remaining four mice were imaged in a 1.5 hour long PET/CT scan, 4.5 hours PI and were sacrificed 6 hours PI. Mice were sacrificed by cervical dislocation and tissue was collected and weighed for macroscopic imaging, scintigraphy, and histological sectioning. Fluorescent organ imaging was performed on tissue in petri dishes immediately following PET/CT scanning using a Bruker Xtreme^{TM} full field fluorescence imaging device. Tissue containing A549 expressing GFP was imaged with excitation/emission of 486/535 nm, respectively, and Cy7 Cetuximab-**2** was imaged with excitation/emission of 730/790 nm, respectively. Tissue was transferred to test tubes and scintillated on a Wallac Wizard 3.0 gamma counter immediately following fluorescence imaging. Following scintillation, tissue was frozen in Optimal Cutting Temperature (OCT) Compound (Sakura Tissue-Tec, #4585) cryogenic embedding medium and analyzed a few days later by cryohistology on an Axiovert 200 fluorescent microscope. Three important observations were noted: 1) Metastases to the lung were not visible through the chest wall, by fluorescence or bioluminescence. This blinded our choice of A549 orthotopic lung tumor bearing mice in 2.5 and 6 hours cohorts, and required *ex vivo*, visual confirmation of orthotopic A549 cells in the lung. A549 metastases were visible in all mice and could be distinguished from normal lung tissue after 6 hours. After 6 hours, there is a statistically significant difference between [^{18}F]-Cetuximab-**2** signal between tumor and lung tissue (Figure S19, S20). 2) The [^{18}F]-Cetuximab-**2** signal in the heart and spleen represent the general blood pool, which decreases over time (2.5 to 6 hours) while the [^{18}F]-Cetuximab-**2** signal in the tumor increased over time. 3) [^{18}F]-Cetuximab-**2** accumulates in the kidneys and liver, which represent different routes of clearance from the blood.

6.5 Data analysis and statistical methods. Fluorescent images were adjusted and analyzed using ImageJ. PET/CT were processed with Amide v1.0.4 and Inveon Research Workplace. Graphs, statistics, and statistical significance tests were generated using Sigmaplot 10.0 (Systat Software Inc.) and KaleidaGraph 4.1 (Synergy). For biodistribution studies, a Kruskal-Wallis Rank Sum Test was used to determine a *P* value from biodistribution data. α was set at 0.05 and a significant difference was observed between [^{18}F]-Cetuximab-**2** tumor and lung tissue uptake at 6 hours. All error bars are standard error of the mean (SEM).

6.5.1 Notes on Fluorescent macro histology. A histological sample that is imaged by a ^{18}F-PET/FL antibody that is distributed systemically and then resected with PET/FL guidance can be used to perform a key experiment that cannot be performed with PET alone. The systemic delivery of a mAb targeted to a tumor helps identify whether the related therapeutic can homogeneously distribute to antigen bearing cells within a histological sample. One would compare the systemic mAb delivery to a tumor site, where the FL probe would identify antigen that can be accessed by an antibody. This will be compared with FL histology obtained through *ex vivo* FL-antibody-staining (which identifies total expressed receptors within a solid tumor, i.e. total antigen content). This comparison would identify the degree of to which a therapeutic equivalent mAb is able to penetrate and deliver itself homogeneously to all expressed receptors within a solid tumor. This information would have a bearing on mAb chemotherapy, and would not be accurately provided by antibody fragments or reengineered antibodies that have very different pharmacokinetic distribution. Such analyses could save money by predicting whether a patient would respond to an expensive antibody therapy.

6.5.2 PET vs. Fluorescent imaging. The signal to noise generated by a fluorophore relative vs. PET emission is related to the time of imaging. At short-time points, PET may generate more signal to noise than a FL, but at longer time points, especially after quantitative isotopic decay, fluorophores generate infinitely more signal than PET emitters (in theory, without considering photo-bleaching, pharmacokinetic FL clearance, or FL metabolism by a biological system). Consider that the energy for PET emission is contained internally, i.e. one photon is emitted from an unstable nucleus before it is transformed into a non-PET element. A fluorophore, on the other hand, draws its energy from an external energy source, and as long as there is an infinite supply of exciting light, a single fluorophore can fluoresce over and over again, generating infinite signal, (at least theoretically, if one does not consider photo-bleaching).

FIGURES

Figure S1. Mal-**1** synthesis and aqueous conversion into the trifluoroborate, Mal-**2**.

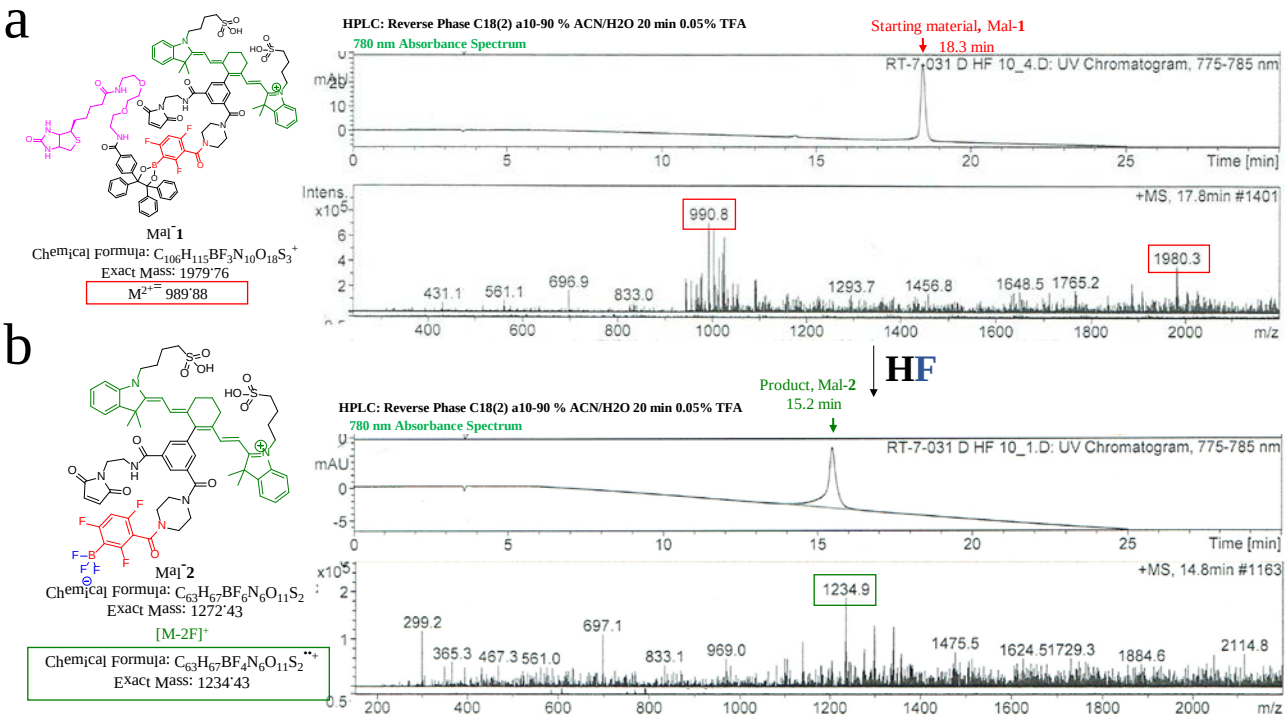

(a) Analytical HPLC-MS of starting material, Mal-**1**. Treatment of Mal-**1** with aqueous HF triggers conversion of the biotinylated NIRF molecule, Mal-**1**, into Mal-**2**. (b) The reaction liberates biotinylated pinacol from the trifluoroborate/NIRF (Mal-**2**) during formation.

Figure S2. Reactions of Mal-**1** with various concentrations of fluoride.

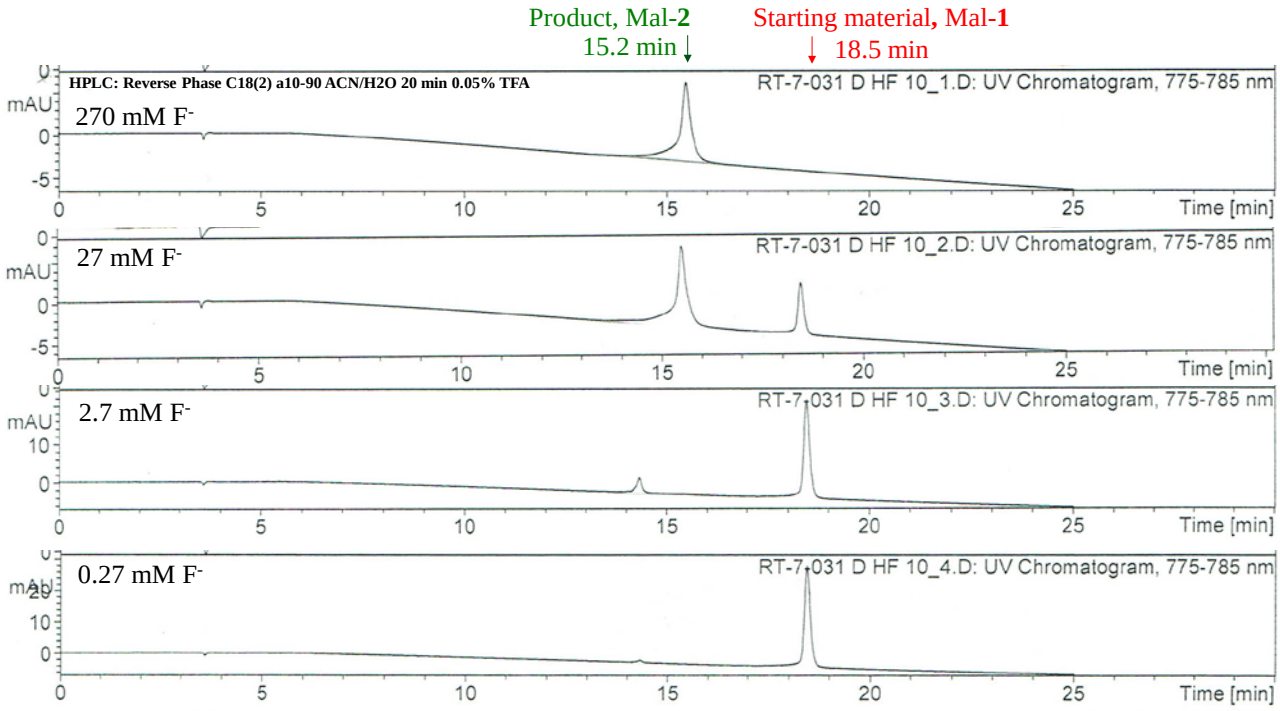

The conversion of Mal-**1** to its trifluoroborate (Mal-**2**) occurs within 2 hours at pH 3 and at concentrations >2.7 mM HF in 50:50 ACN:H_2O.

Figure S3. Fluorescence imaging of Mal-**1**-biotin capture on magnetic streptavidin-IO (str-IO) particles (pH 7.4).

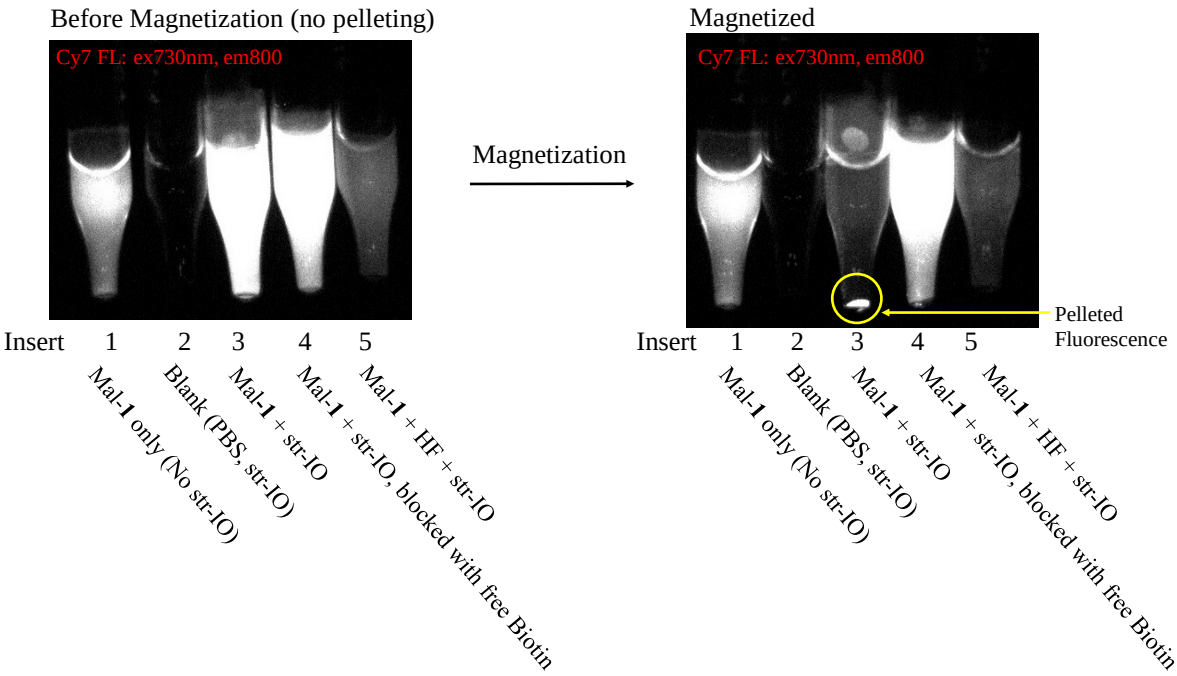

Mal-**1** pelleted fluorescence in DPBS (pH 7.4) is not observed (Insert 1). DPBS shows no auto-fluorescence (Insert 2). Mal-**1** fluorescence is pelleted by a magnetic field because biotin binding to streptavidin-IO particles (Insert 3). Pelleted fluorescence is prevented with excess of free biotin (Insert 4) or when the biotin handle is removed by converting Mal-**1** into Mal-**2** with HF (Insert 5). These experiments indicate the biotin-specific capture of Mal-**1** on streptavidin-IO.

Figure S4. Fluoride triggered elution of Mal-**2** from Mal-**1** bound streptavidin-agarose**.**

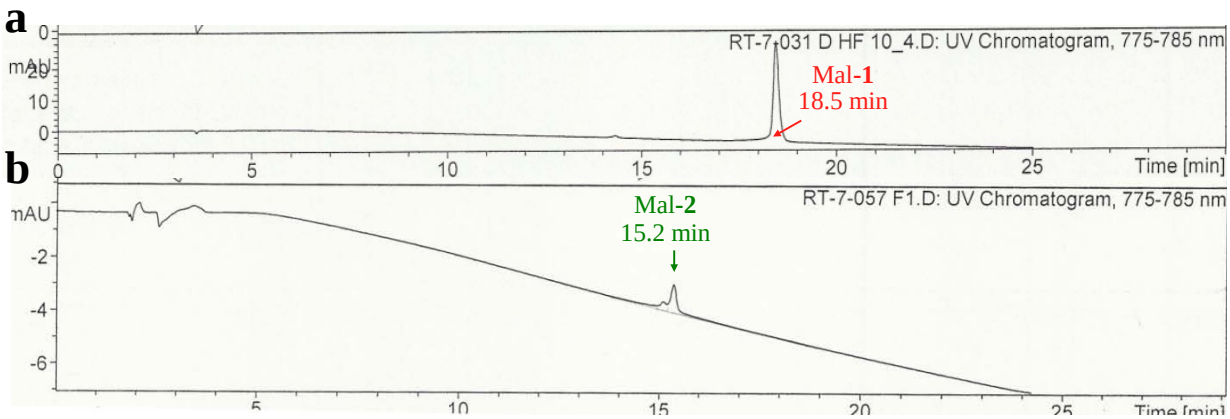

(a) Reverse phase HPLC of starting material, Mal-**1**, before it is bound to streptavidin-agarose and reacted with HF. (b) Mal-**1** was bound to streptavidin-agarose, HF was added for 40 min, and the eluent was collected and directly analyzed by HPLC. The eluent contains only Mal-**2** and is only 5-10% of the total Mal-**1** loaded onto the column.

Figure S5. SEC HPLC analyses of mAb and mAb-**1**.

a

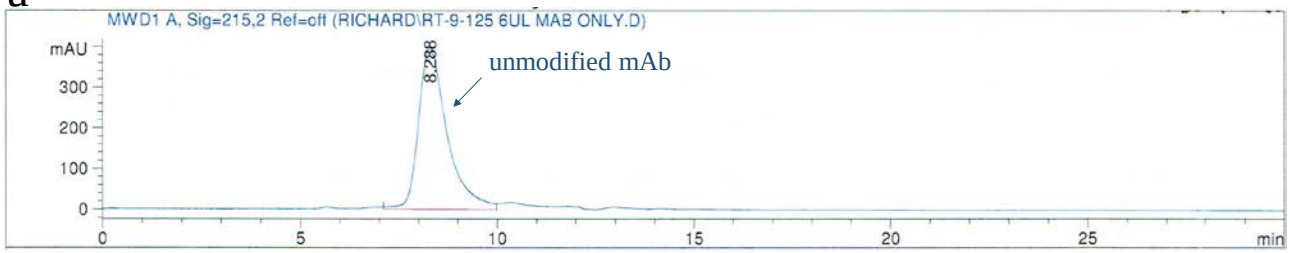

b

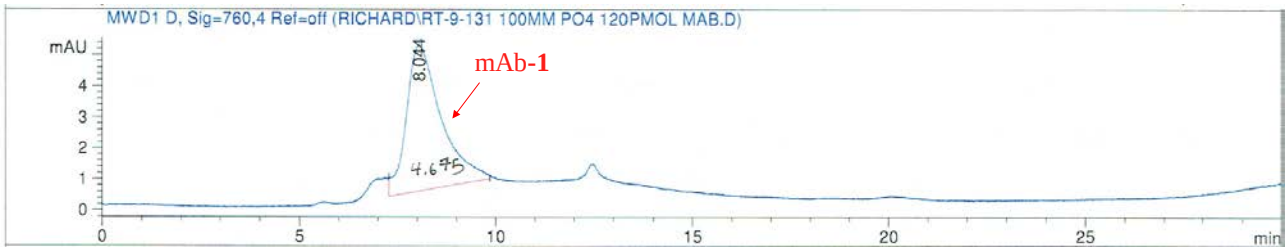

(a) 215 nm absorbance SEC elution profile of unconjugated mAb. (b) SEC elution profile of mAb-**1** using 760 nm absorbance. SEC HPLC, with these conditions, is unable to separate mAb-**1** from unconjugated mAb.

Figure S6. PAGE gel demonstrates mAb-**1** binding to streptavidin-agarose**.**

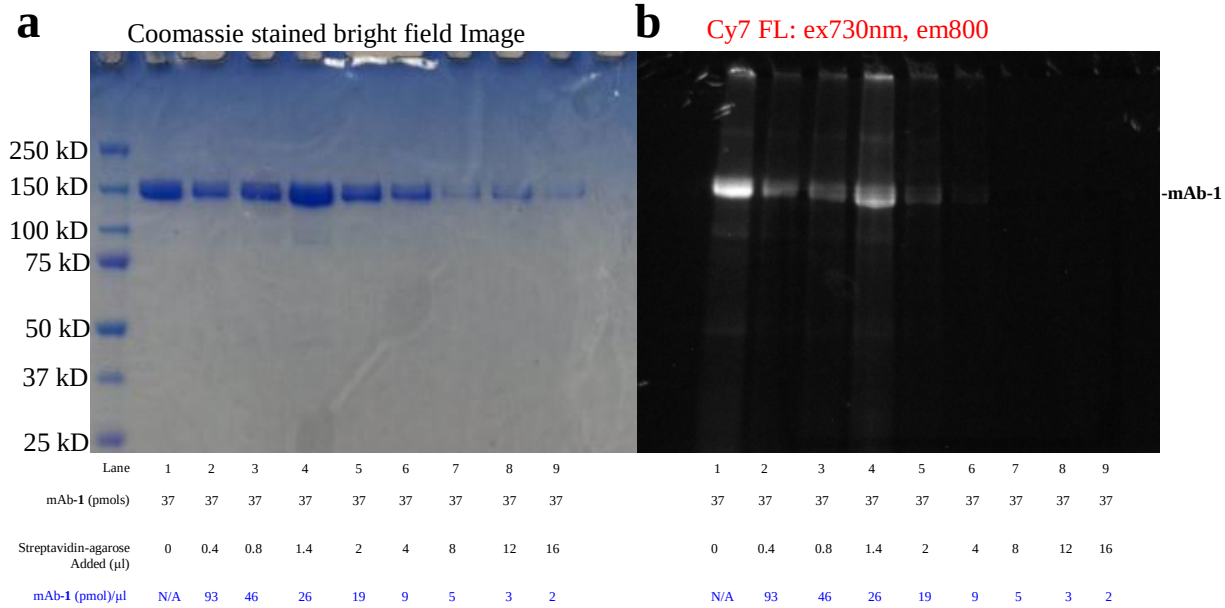

(a) Coomassie stain shows total protein (mAb and mAb-**1**). (b) Cy7 fluorescence imaging shows only biotin-bearing, mAb-**1**. By increasing the titer of streptavidin-agarose, mAb-**1** becomes completely bound to streptavidin-agarose. At larger volumes of streptavidin-agarose, mAb-**1** fluorescence is not observed because it remains bound to streptavidin-agarose (retained on cellulose acetate filters) (Lanes 5-9). 37 pmols of mAb-**1** is completely bound by 2-4 µl streptavidin-agarose.

Figure S7. Coomassie stained gel demonstrating the lack of non-specific binding between unreacted mAb and streptavidin-agarose.

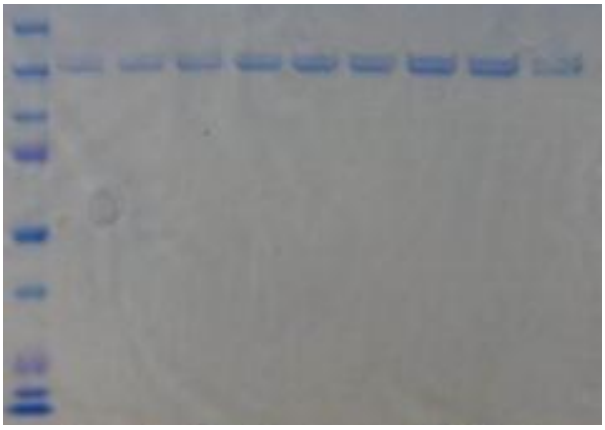

Lane:	1	2	3	4	5	6	7	8	9
Added streptavidin agarose (µL):	0	1	2	4	8	12	16	24	32

Non-specific binding between streptavidin-agarose and unlabeled mAb (20 pmol) is not observed. If significant mAb bound streptavidin-agarose, there would be reduced mAb coomassie staining at increased quantities of streptavidin-agarose.

Figure S8. HPLC confirmation of the quantitative conversion of **1** into its trifluoroborate, **2**.

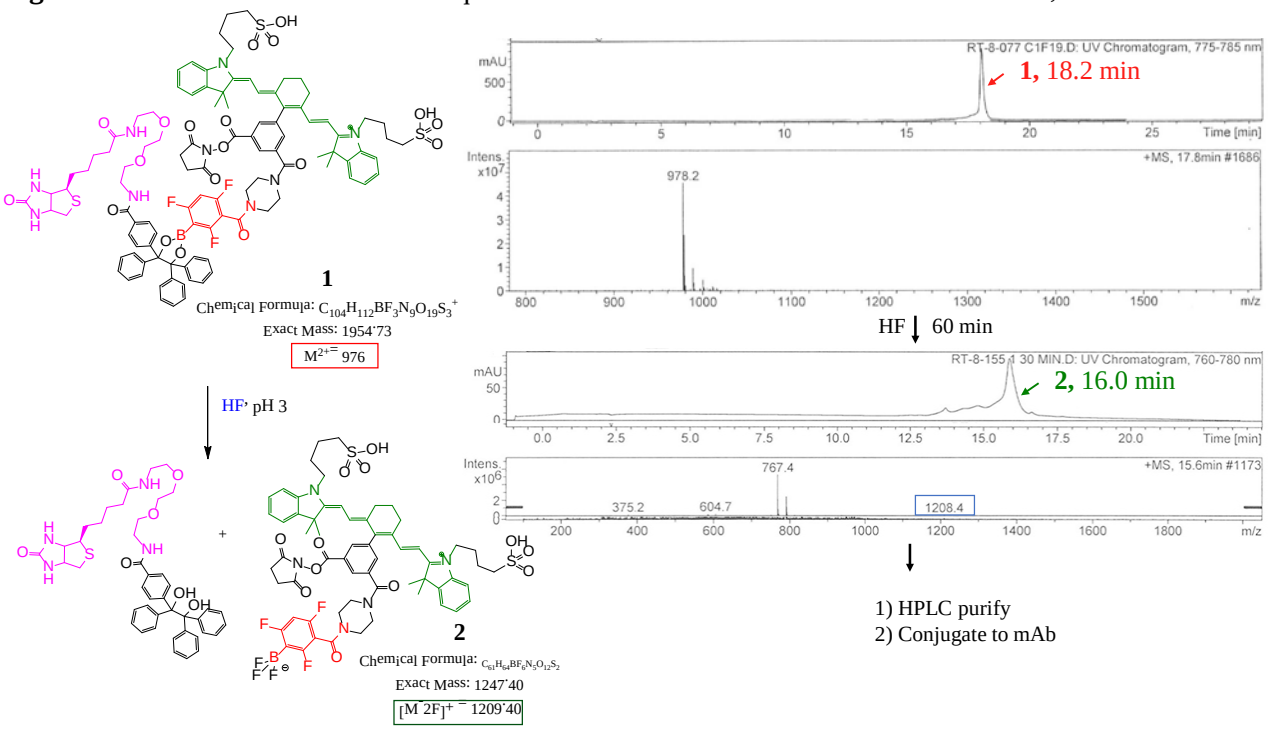

An aliquot of **1** was reacted with HF to quantitatively give **2**. This synthetic scheme is less suited for the [^{18}F]-radiosyntheses of [^{18}F]-mAb-**2** because of the additional step required and purification of [^{18}F]-mAb-**2** from the biotinylated pinacol.

Figure S9. SDS-PAGE gel of mAb-**2** demonstrating a lack of binding between 37 pmols mAb-**2** and streptavidin-agarose.

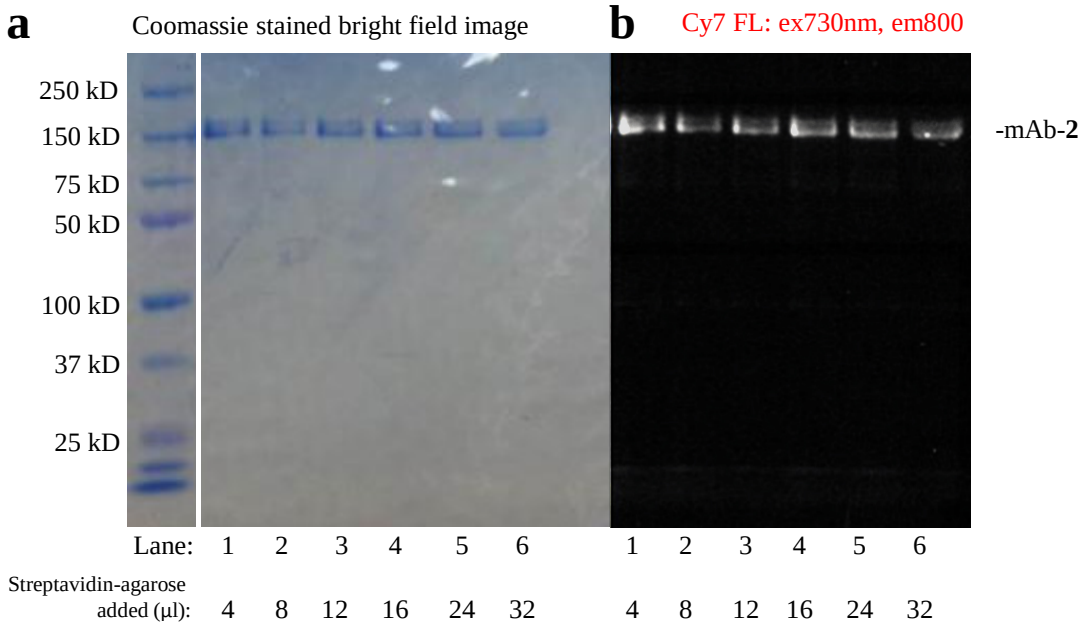

(a) Coomassie stained gel showing equal loading of mAb-**2**. (b) Cy7 fluorescence image showing equal amounts of mAb-**2** eluted from the streptavidin-agarose in all preparations. The lack of variation in mAb-**2** coomassie and fluorescence show that non-specific binding is not observed between mAb-**2** and streptavidin-agarose.

Figure S10. SEC HPLC elution profile of mAb-**1** reacted at room temperature for 130 min with aqueous [^{18}F]-fluoride.

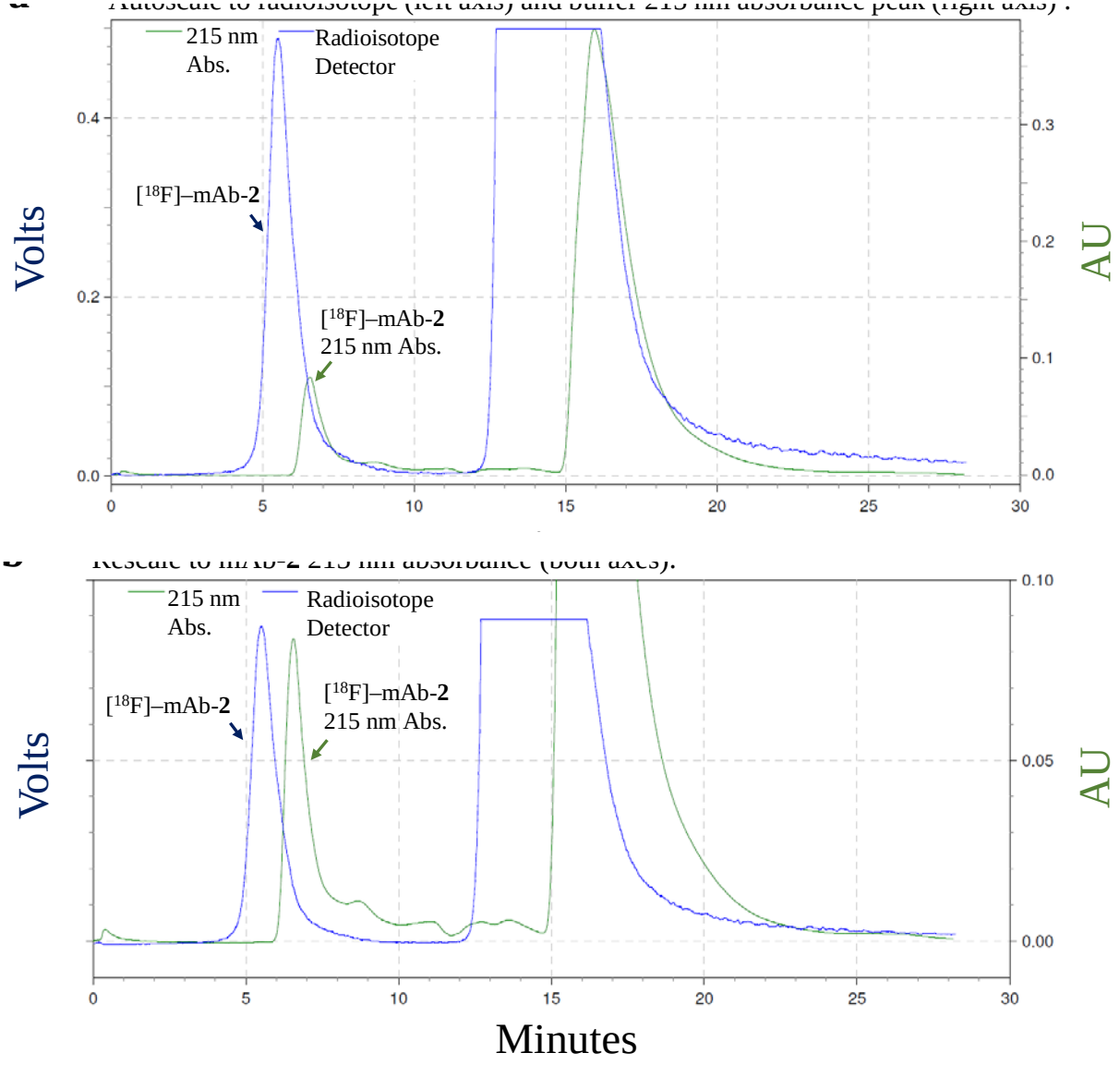

No streptavidin-agarose was used in this synthesis of mAb-**2** (Scheme S4a). SEC HPLC absorbance at 215 nm was acquired on a System Gold 166 Detector (shown in green). A Beckman 170 Radioisotope detector was used to monitor radioactivity (offset blue trace). The offset is -1.5 min and confirmed by scintillation counting. [^{18}F]-mAb-**2** elutes at 5-7 min with a 215 nm absorbance of 83.2 mAU (absorbance units). [^{18}F]-fluoride elutes after 13 min. (a) Unscaled SEC HPLC data. (b) Normalized SEC HPLC data.

Figure S11. SEC HPLC analysis of the supernatant resulting from the reaction of mAb-**1** with aqueous [^{18}F]-fluoride, followed by a work up with streptavidin-agarose.

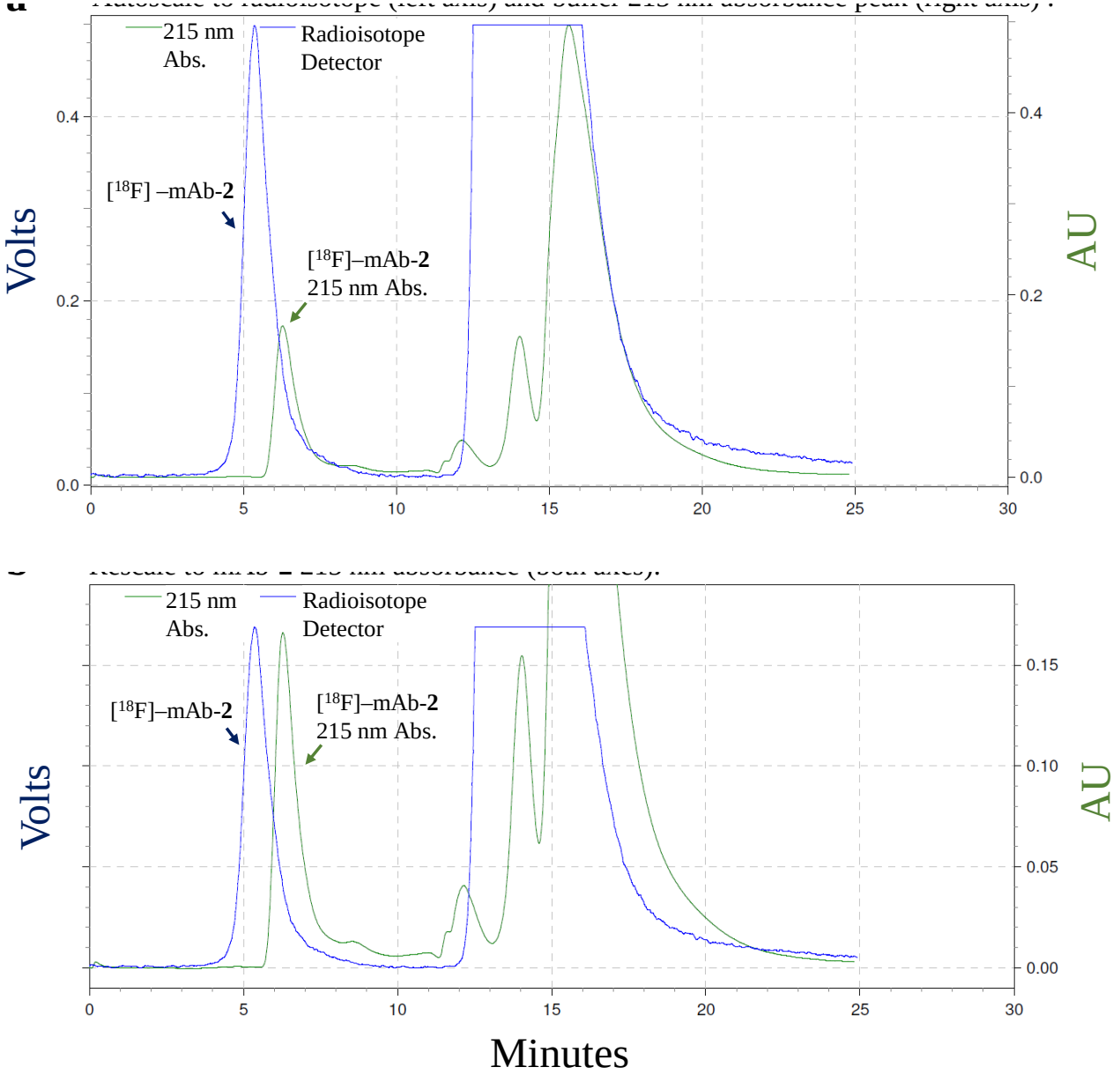

The fluoridation products are a mixture of [^{18}F]-mAb-**2** and unreacted mAb (Scheme S4b). Absorbance at 215 nm is shown in green. Radioactivity data is shown in the offset blue trace. [^{18}F]-mAb-**2** elutes at 5-7 min with a 215 nm absorbance of 162 mAU. [^{18}F]-fluoride elutes between 12-18 min. (a) Unscaled SEC HPLC data. (b) Normalized SEC HPLC data.

Figure S12. SEC HPLC analysis of the eluent generated from mAb-**1** bound to streptavidin-agarose reacted with [^{18}F]-fluoride.

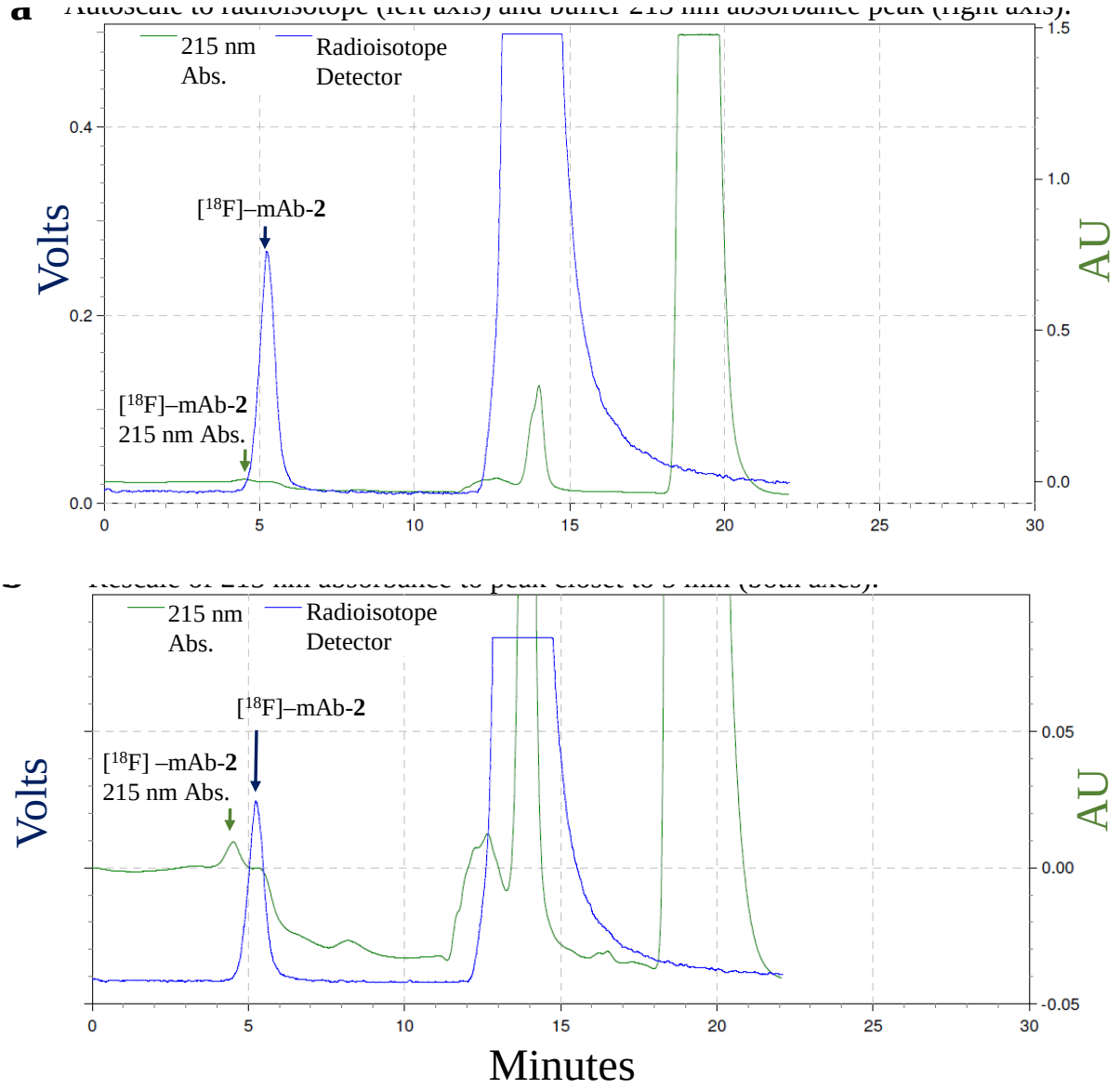

mAb-**1** bound to streptavidin-agarose was reacted with aqueous [^{18}F]-fluoride to elute [^{18}F]-mAb-**2**. The eluent was collected by centrifugation, loaded on a SEC HPLC, and analyzed with a 215 nm absorbance detector (green) and a radioisotope detector (blue). The eluent contains only [^{18}F]-mAb-**2** (Scheme S4c). (a) Unscaled raw SEC HPLC data. Note a 13-fold SA enhancement reflected by the increased ratio of radioactivity (blue) to reduced 215 nm absorbance of [^{18}F]-mAb-**2** relative to Figure S10. Data from (b) (normalized SEC HPLC data) was used to calculate SA enhancement by streptavidin-agarose. In this case, the largest 215 nm absorbance at 4.5 min was assumed to correspond to [^{18}F]-mAb-**2**.

Figure S13. SEC HPLC analysis demonstrating the lack of non-specific binding/labeling between unmodified mAb and [^{18}F]-fluoride.

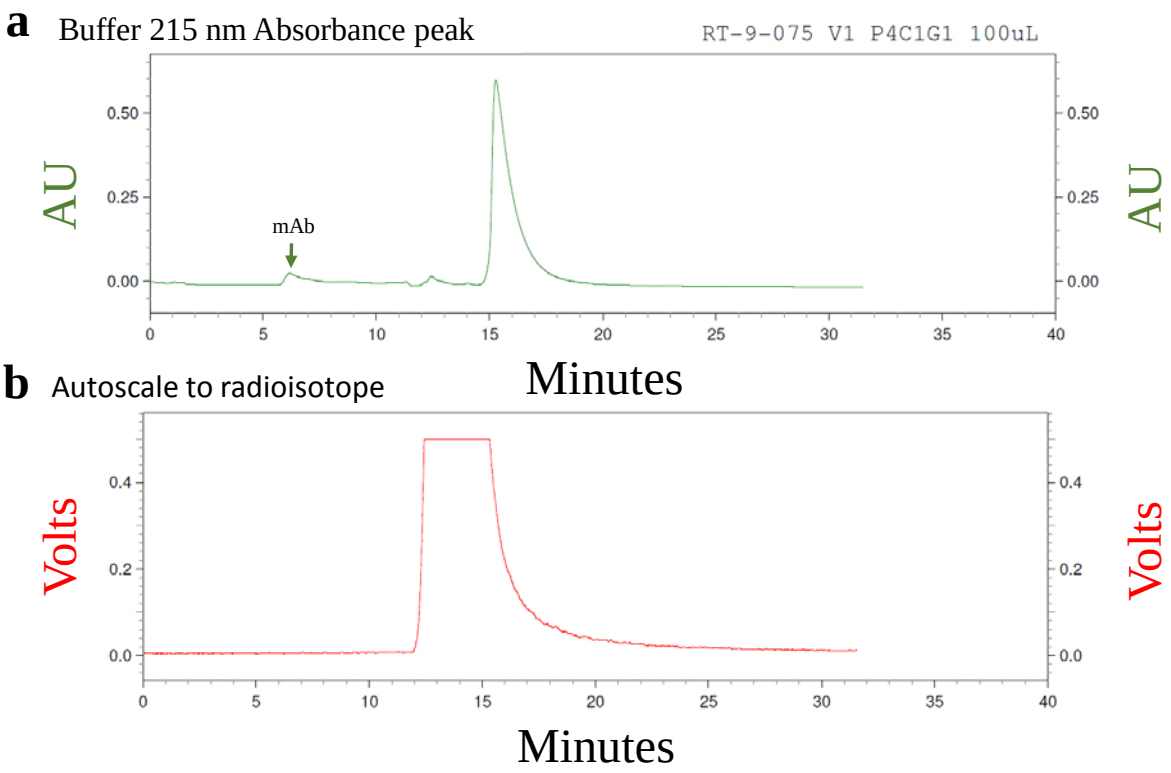

No binding/labeling was observed between unmodified mAb and [^{18}F]-fluoride. (a) 215 nm absorbance detector data (green). (b) Radioisotope detector data (red).

Figure S14. Comparison of relative specific activities for different preparations of mAb-**2**.

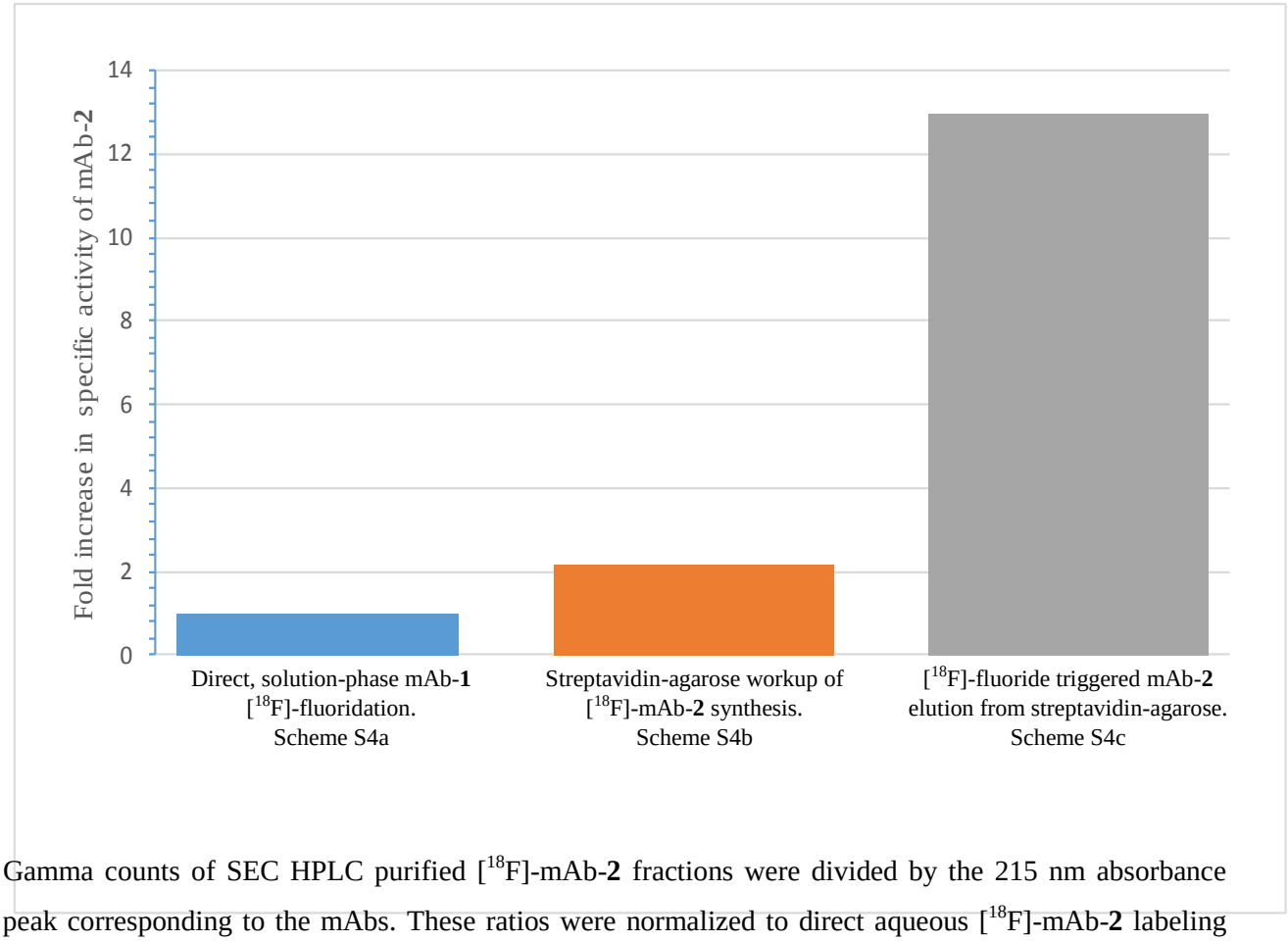

Gamma counts of SEC HPLC purified [^{18}F]-mAb-**2** fractions were divided by the 215 nm absorbance peak corresponding to the mAbs. These ratios were normalized to direct aqueous [^{18}F]-mAb-**2** labeling without streptavidin-agarose workup. There is a clear enhancement in specific activity with the use of streptavidin-agarose in the preparation of [^{18}F]-mAb-**2**.

Figure S15. SDS PAGE gel of the chemical reduction of mAb-**2** into fragments.

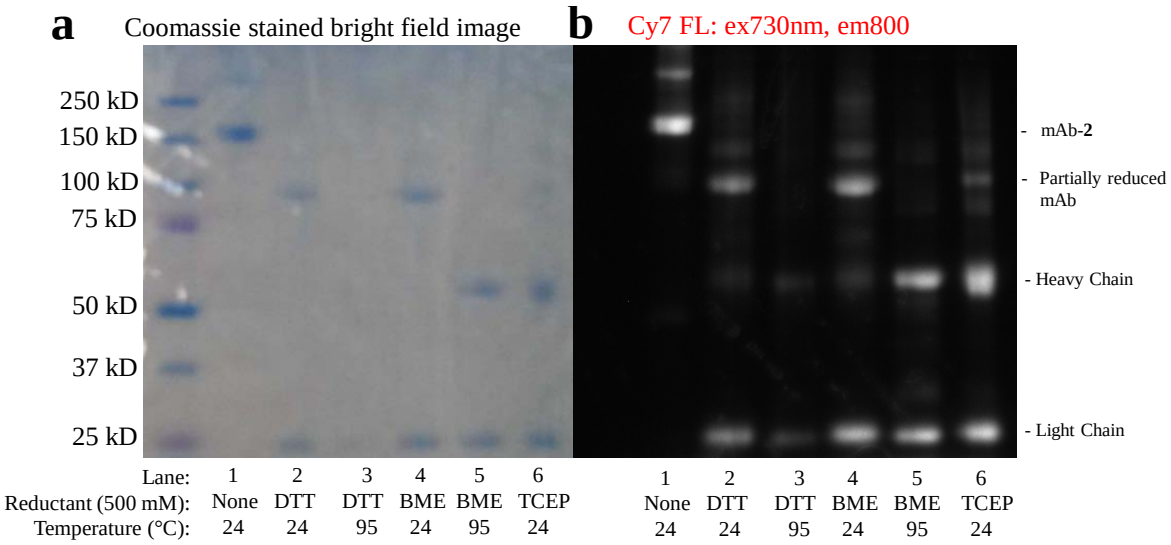

mAb-**2** was reduced with dithiothreitol (DTT), β-mercaptoethanol (BME), or 3,3',3"-Phosphanetriyltripropanoic acid (TCEP). Reductions were allowed to proceed for 2 hours at room temperature or 95 °C. (a) Coomassie stained gel showing total protein. (b) Fluorescence imaging confirms a functional Cy7 fluorophore. BME at 95 °C or TCEP at room temperature were the best conditions for reducing mAb-**2** into heavy and light chains and retaining Cy7 fluorescence.

Figure S16. Viable and heat-denatured mAb-**2** imaging of PC3-DsRed2 tumor xenografts in mice.

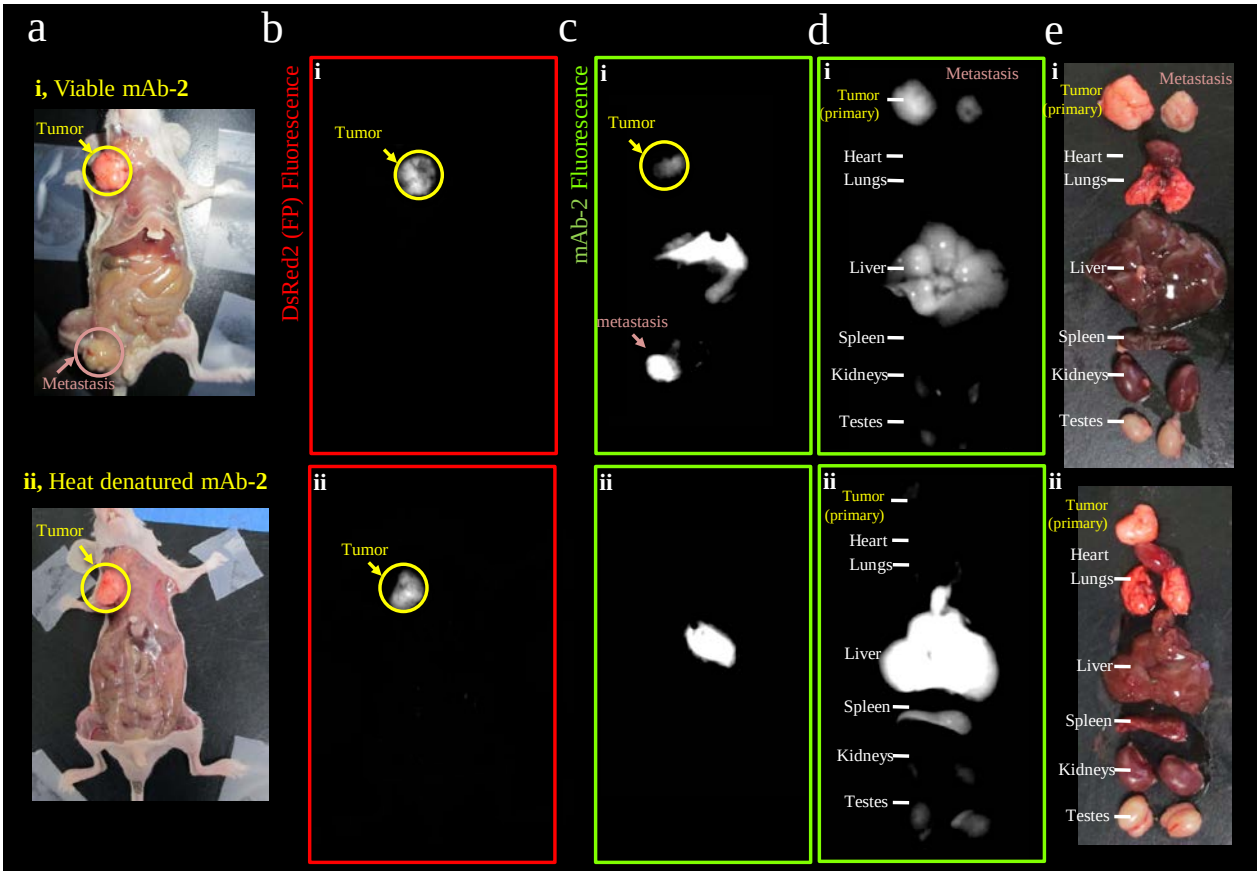

(a) Brightfield images of two different mice bearing PC3 tumors expressing DsRed2 at 72 hours. (i) Mouse injected with mAb-**2** (600 pmol) and (ii) a mouse injected with heat-denatured mAb-**2** (600 pmol). (b) DsRed2 fluorescence imaging of PC3 primary tumors expressing DsRed2. (c) mAb-**2** fluorescence imaging demonstrating (i) mAb-**2** accumulation at the tumor (note: metastasis is observed only in the Cy7 channel in the lower right quadrant with mAb-**2**) and (ii) lack of tumor accumulation when mAb-**2** is heat-denatured. (d) *Ex vivo* Cy7 fluorescence organ images confirming (i) mAb-**2** accumulates in the primary and metastasized tumors, and (ii) that mAb-**2** does not accumulate at tumors when mAb-**2** is heat-denatured. (e) *Ex vivo* bright field images of resected organs containing (i) viable mAb-**2** and ii) denatured mAb-**2**.

Figure S17. Flow cytometry analysis of Cetuximab-**1/2** binding to EGFR expressed on A549 cells after various fluoridation concentrations (pH 3).

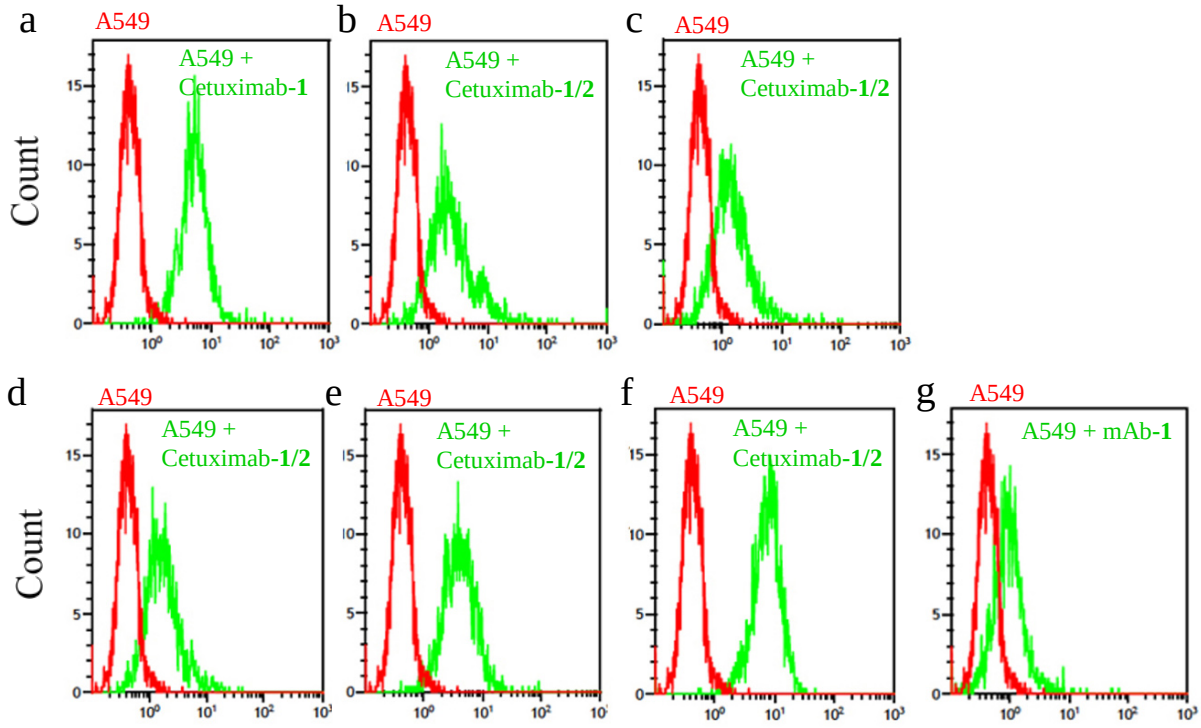

A549 cells were incubated with no Ab (red) or with Ab (green). (a) (Control 1) Cetuximab-**1** stored at pH 7.5 binds EGFR on A549 cells. Cetuximab-**1** was fluoridated for 2 hours with the following acid concentrations: (b) 2,000 mM HF and 0 mM HCl, (c) 333 mM HF and 111 mM HCl, (d) 111 mM HF and 111 mM HCl, (e) 37 mM HF and 37 mM HCl, and (f) 12 mM HF and 12 mM HCl. (g) A549 cells express little EpCAM on the membrane surface. (Control 2) mAb-**1** (EpCAM) was incubated with A549 cells. All fluoride treated Cetuximab-**1/2** samples (a-f) show greater fluorescence than mAb-**1** EpCAM. Cetuximab-**1/2** notation is used in cases where streptavidin-agarose was not used to remove unreacted Cetuximab-**1** from Cetuximab-**2**.

Figure S18. A549 primary and metastatic lung tumor confirmation and lung focused PET/CT.

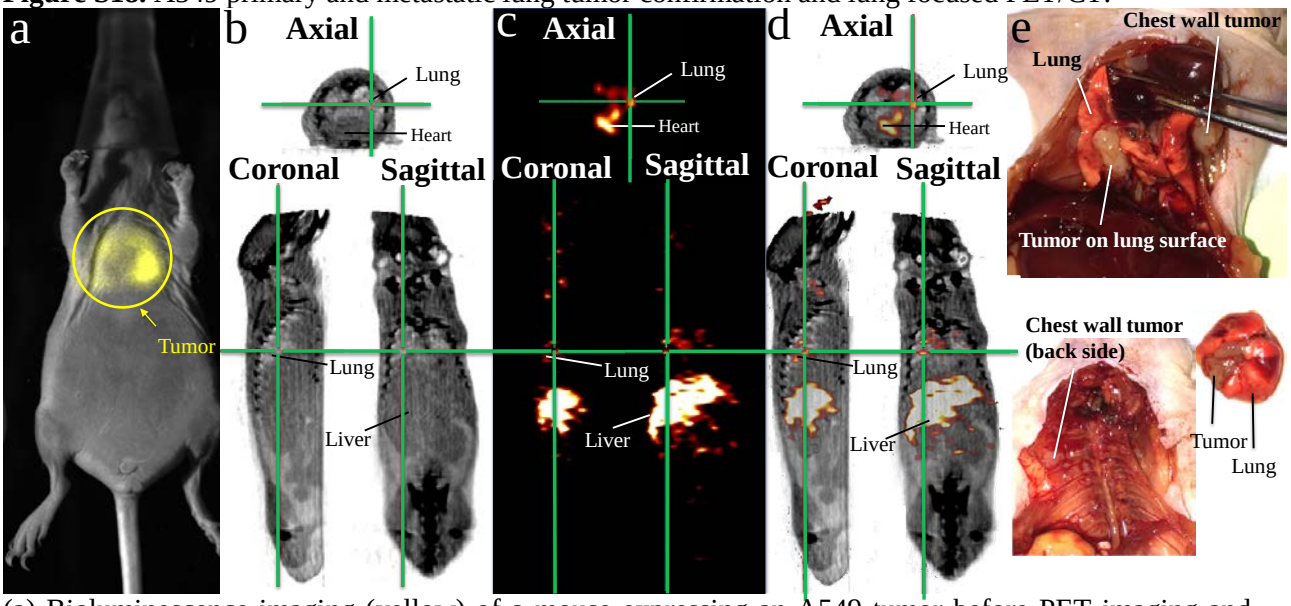

(a) Bioluminescence imaging (yellow) of a mouse expressing an A549 tumor before PET imaging and dissection. (b) CT, (c) PET, and (d) Overlay PET/CT images (axial, coronal, and sagittal) of [^{18}F]-Cetuximab-**2** in the lung of a mouse that has an A549 primary tumor. (e) Dissection following PET imaging showing primary tumor growth on the chest wall and metastasis into the lung.

Figure S19. Tumor focused PET/CT imaging and tissue biodistribution data confirming [^{18}F]-Cetuximab-**2** signal in orthotopic A549 tumor.

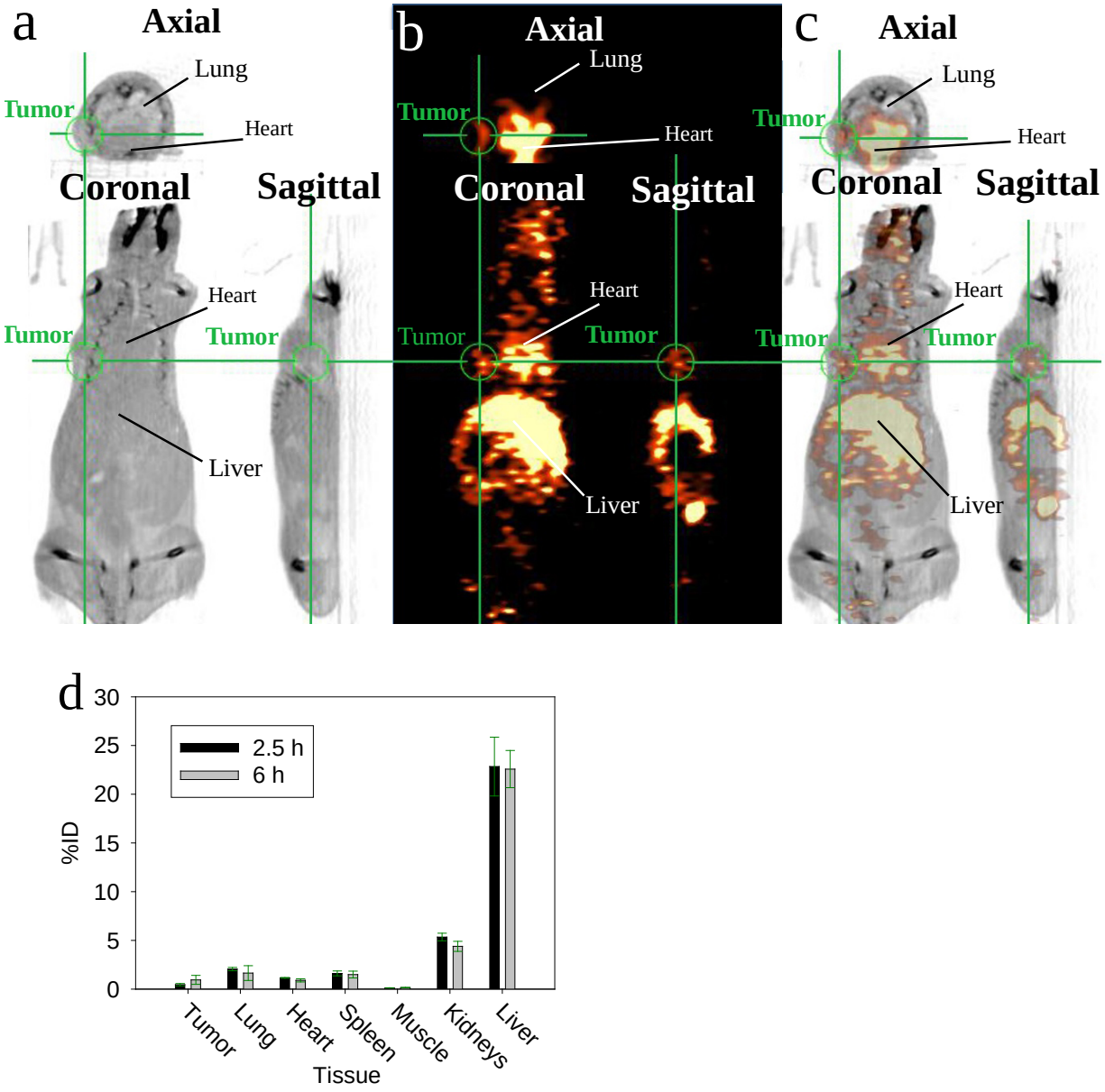

(a) CT, (b) PET, and (c) PET/CT images (axial, coronal, and sagittal) focused on an orthotopic A549 primary tumor (green crosshairs) taken 6 hours after [^{18}F]-Cetuximab-**2** injection. (d) Percentage of injected dose (% ID) in tissue calculated from scintillated, *ex vivo* biodistribution at 2.5 (n = 3) and 6 (n = 4) hours.

Figure S20. ROI analyses of mice in Figure 6g. Spherical, 2 mm^3 ROI were placed over different tissue in order to generate SUV analyses for bone distribution and tumor/non-tumor uptake.

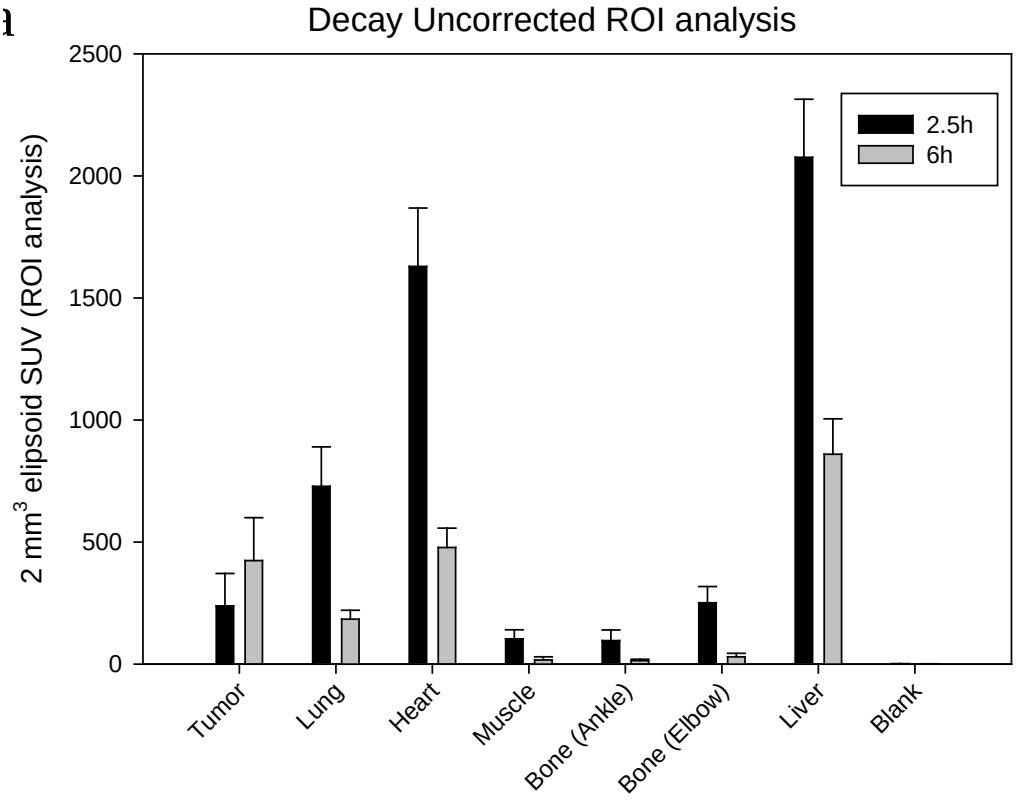

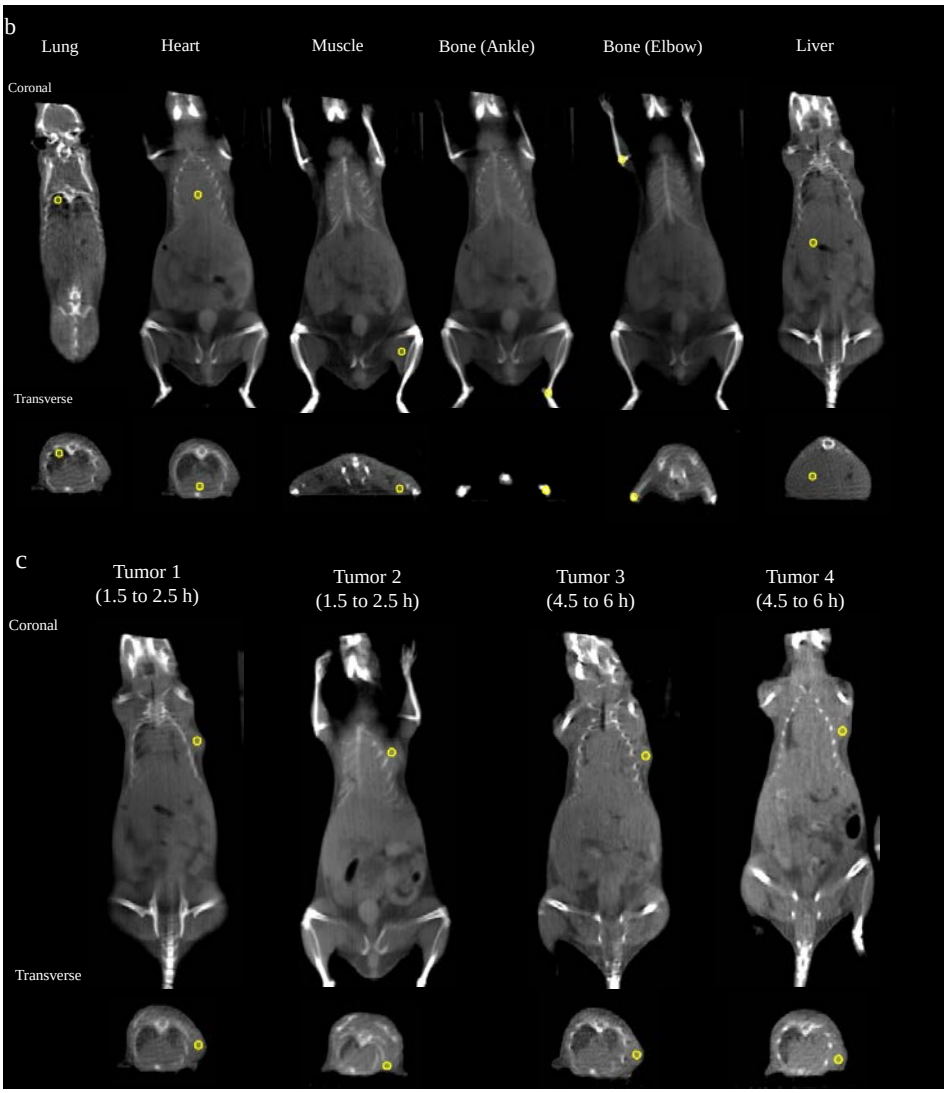

PET/CT scans of mice in Figure 6 were additionally analyzed in decay uncorrected ROI analyses. (a) Decay uncorrected ROI analysis (with standard error) of PET activity in mice that were injected with [^{18}F]-Cetuximab-**2**. Analyses were performed on static reconstructions of images between 1.5 to 2.5 (n = 3) and 4.5 to 6 hours (n = 4) (b) CT demonstrating placement of 2 mm^3 ellipsoid ROIs (yellow) over analyzed tissue. (c) CT demonstrating placement of ROI over observable tumor xerographs. Note that tumor n = 2 in 1.5-2.5 hours cohort and n = 3 in 4.5-6 hours cohort as tumors were not all obvious in all CT. This is accounted for in standard error calculations (Error = $\sigma/(n^{1/2})$). Bone uptake is low relative to tumor and non-tumor tissue. Bone signal may be a sum of dissociated ^{18}F-ion and [^{18}F]-Cetuximab-**2**, as bone is vascularized. Tumor to non-tumor signal is greater in the 4.5-6 hour scan. This ROI is superior for calculating heart biodistribution (vs. scintillated biodistribution) as heart changes its volume after removal

from the body. ‘Blank’ SUVs correspond to 2 mm^3 ellipsoid volumes measured outside of mice between mice. They are 1.3 ± 0.5 SUV for the 1.5-2.5 hours analysis and 0.5 ± 0.4 SUV 4.5-6h analysis.

Video S1. Sample PET/CT scan of [^{18}F]-Cetuximab-**2** dosing study in four mice bearing immature A549 lung tumors. Images were acquired 4.5-5 hours post i.v. injection as described for Figure 6. PET is shown in orange and CT is show in gray.

Video S2. PET scan of [^{18}F]-Herceptin-**2** in four mice bearing immature A549 lung tumors prepared using the Cetuximab labeling procedure. Images were acquired 4.5-5 hours post i.v. injection.

SUPPORTING REFERENCES

(44) Lee, H., Mason, J. C., and Achilefu, S. (2006) Heptamethine cyanine dyes with a robust C-C bond at the central position of the chromophore. *J. Org. Chem. 71*, 7862-7865.

(45) Kirkpatrick, P., Graham, J., and Muhsin, M. (2004) Cetuximab. *Nat. Rev. Drug Discov. 3*, 549-550.

(46) Derer, S., Bauer, P., Lohse, S., Scheel, A. H., Berger, S., Kellner, C., Peipp, M., and Valerius, T. (2012) Impact of epidermal growth factor receptor (EGFR) cell surface expression levels on effector mechanisms of EGFR antibodies. *J. Immunol. 189*, 5230-5239.

(47) Mordant, P., Loriot, Y., Lahon, B., Castier, Y., Leseche, G., Soria, J. C., Vozenin, M. C., Decraene, C., and Deutsch, E. (2011) Bioluminescent orthotopic mouse models of human localized non-small cell lung cancer: feasibility and identification of circulating tumour cells. *PLoS One 6*, e26073.